# 1. Leg 198 Synthesis: A Remarkable 120-m.y. Record of Climate and Oceanography from Shatsky Rise, Northwest Pacific Ocean[1]

Timothy J. Bralower,[2] Isabella Premoli Silva,[3] and
Mitchell J. Malone[4]

## ABSTRACT

Samples collected from a depth transect of eight sites during Ocean Drilling Program Leg 198 to Shatsky Rise contain a remarkable sedimentary record of surface and deepwater circulation in the tropical Pacific over the past 120 m.y. In addition, basement sills recovered provide valuable constraints on the age and origin of the volcanic foundations of the rise.

The sediments recovered contain evidence of the long-term transition from greenhouse to icehouse climate state and of several abrupt climate change events. Shatsky Rise cores contain an exceptional record of an Oceanic Anoxic Event (OAE1a) in the early Aptian (120 Ma), with some of the highest organic carbon contents measured in pelagic sediments. These strata contain exceptionally preserved organic compounds including the oldest known alkenones. Organic geochemistry suggests that bacterial activity played a significant role in sequestering organic carbon. Stable isotope data from Upper Cretaceous and Paleogene sediments reveal several abrupt switches in the sources of intermediate waters bathing Shatsky Rise. Neodymium isotopes also show evidence for these changes and help to identify source regions in the North Pacific, Southern Ocean, and, possibly, Tethys.

Strong evidence exists in Shatsky cores for the mid-Maastrichtian (~69 Ma) global extinction of inoceramids, a long-ranging, widespread group of bottom-dwelling clams. Stable and neodymium isotopes com-

[2]Department of Geosciences, Pennsylvania State University, University Park PA 16802, USA.
**bralower@geosc.psu.edu**
[3]Dipartimento di Scienze della Terra, Università degli Studi di Milano, Via Mangiagalli 34, 20133 Milano, Italy.
[4]Ocean Drilling Program, Texas A&M University, 1000 Discovery Drive, College Station TX 77845-9547, USA. Present address: Integrated Ocean Drilling Program, Texas A&M University, 1000 Discovery Drive, College Station TX 77845-9547, USA.

bined with biotic data show changes in intermediate water sources at this time as well as significant changes in surface water oceanography. Shatsky Rise sites contain high-quality records of the Cretaceous/Tertiary boundary event. Detailed nannofossil assemblage studies demonstrate that the survivor taxa are those that were adapted to unstable environmental conditions of shelves, including taxa that have cyst stages. The Paleogene sedimentary record from Shatsky Rise is strongly cyclic with variations in the amount of dissolution. Superimposed on this record are "hyperthermal" episodes including the Paleocene/ Eocene Thermal Maximum (PETM; ~55.0 Ma) and events in the early late Paleocene (~58.4 Ma) and early Eocene (52.7 Ma). The PETM on Shatsky Rise contains evidence for 5°C warming of tropical sea-surface temperatures, major reorganization of benthic and planktonic communities, and pronounced short-term shoaling of the lysocline. Oxygen isotope and Mg/Ca data demonstrate warming of surface and intermediate waters (possibly combined with decreasing salinity) during the early Eocene and help constrain the timing of the acceleration of Antarctic glaciation during the middle Eocene.

Recovery of basaltic sills provides valuable age and geochemical constraints for interpreting the origin of Shatsky Rise. Radiometric ages confirm previous suggestions that this large igneous province was emplaced rapidly. Isotope geochemistry shows a mid-ocean-ridge basalt signature that argues against a mantle plume origin. However, alternative origins are difficult to prove unequivocally.

# INTRODUCTION

The sedimentary record recovered over the course of several decades of deep-sea drilling has yielded a wealth of information on Earth's climate system. Pelagic sedimentary sections provide some of the most faithful time series of climate states from the Middle Jurassic to the Holocene. Potentially more significant, however, are the clues within the sedimentary archives of the mechanisms and processes that drive climate change and the effect of that change on biotic evolution and geochemical cycling (e.g., Schlanger et al., 1987; Dickens et al., 1995; Leckie et al., 2002).

The early decades of deep-sea drilling, largely associated with the Deep Sea Drilling Project (DSDP), involved a great deal of exploratory coring in locations where the stratigraphy of the sedimentary section was undocumented and poorly constrained. More recently, however, knowledge from previous drilling expeditions combined with the availability of high-resolution multichannel seismic reflection data have allowed us to target particular time slices at locations where the sedimentary section looks essentially complete. In addition, hydraulic piston coring technology developed during the Ocean Drilling Program (ODP) allows us to obtain high-quality records when these locations are revisited.

Shatsky Rise, a medium-sized large igneous province (LIP) in the west-central Pacific (Fig. F1) was the target of three DSDP expeditions, Legs 6, 32, and 86, and ODP Leg 132 (Fischer, Heezen et al., 1971; Larson, Moberly, et al., 1975; Heath, Burkle, et al., 1985; Natland, Storms, et al., 1993). The quality of the records from the older legs was hampered by rotary and spot-coring as well as low recovery in the Cretaceous because of the presence of persistent chert. Yet these legs revealed the potential of Shatsky Rise sediments to provide high-quality records

**F1.** Bathymetric map of Shatsky Rise, p. 26.
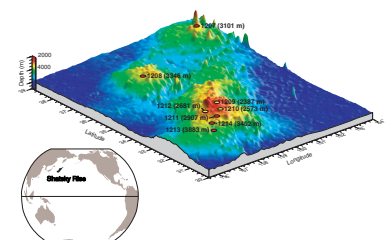
of Cretaceous and Paleogene climate. This interval is located at shallow burial depths on the rise and thus is relatively unaltered by burial diagenesis (e.g., Schlanger and Douglas, 1974). Leg 198 was designed to recover high-quality sedimentary records of this age along a depth transect (Bralower, Premoli Silva, Malone, et al., 2002). The transect has the potential to provide two-dimensional reconstructions of ocean temperature, chemistry (i.e., carbonate solubility and oxygenation), circulation, and biology through some of the most fundamentally interesting intervals of climate change during the entire Phanerozoic.

The mid-Cretaceous (~120–80 Ma) and early Paleogene (~60–45 Ma) were characterized by equable climates including low latitudinal thermal gradients, lack of extensive cryosphere, a relatively warm deep ocean, and high atmospheric $pCO_2$ levels (Fig. F2) (e.g., Barron and Washington, 1985; Berner, 1994). These "greenhouse" intervals also contain significant abrupt and transient warming events that led to major changes in oceanic environments, profound turnovers in marine communities including extinctions, and perturbations to global chemical cycles. Examples include the Paleocene/Eocene Thermal Maximum (PETM) (e.g., Kennett and Stott, 1991; Dickens et al., 1995; Katz et al., 1999; Norris and Röhl, 1999) and Cretaceous Oceanic Anoxic Events (OAEs) (e.g., Schlanger and Jenkyns, 1976; Jenkyns, 1980; Arthur et al., 1985, 1988). Leg 198 was designed to understand the causes, nature, and mechanics of the long-term Cretaceous and Paleogene "greenhouse" as well as of the transient events during this period. The location of Shatsky Rise in the tropical Pacific during the interval of interest is fundamentally significant—the aerial extent and importance of the Pacific in global circulation make this a critical target for investigation of warm climatic intervals. Yet, this ocean basin contains far less complete records than the Atlantic, Indian, and Tethyan Oceans. During Leg 198, one site was drilled on each of the North and Central Highs of Shatsky Rise (Sites 1207 and 1208, respectively) and six sites were drilled on the Southern High (Sites 1209–1214) (Bralower, Premoli Silva, Malone, et al., 2002).

An impressive 140-m.y. package of pelagic sediment was recovered at the eight sites (Figs. F3, F4, F5, F6, F7, F8, F9). In addition, the first cores from the basement of Shatsky Rise were recovered at Site 1213. Detailed descriptions and preliminary interpretations of the cores are provided in Bralower, Premoli Silva, Malone, et al. (2002) and Bralower et al. (2002). A broad array of exciting investigations have been conducted on the Leg 198 cores, resulting in a number of publications in the open literature and in this volume. This summary is organized in terms of the chronological history of Shatsky Rise, beginning with eruption of its basement foundation and followed by the progressive deposition of its sedimentary carapace.

# CONSTRAINTS ON THE ORIGIN OF SHATSKY RISE

At Site 1213, a series of at least three basaltic sills with a total thickness of 46 m was recovered at the base of the sedimentary section. The units underlie limonitic breccias, evidence for hydrothermal activity associated with sill intrusion. The sills are interpreted as a widespread plutonic event associated with the latest stages in the construction of the Southern High of Shatsky Rise. Sediment interbedded in the sills yields

F2. Generalized climate curve for Cretaceous and Paleogene, p. 27.
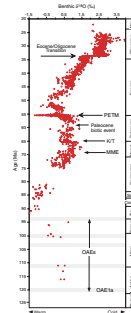
F3. Stratigraphy and lithology, Sites 1207–1214, p. 28.
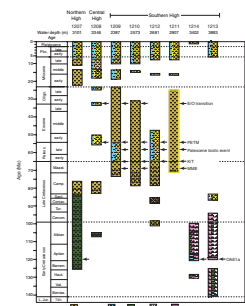
F4. Stratigraphic summary for 145–130 Ma, p. 29.
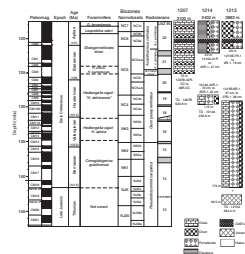
F5. Stratigraphic summary for 130–80 Ma, p. 30.
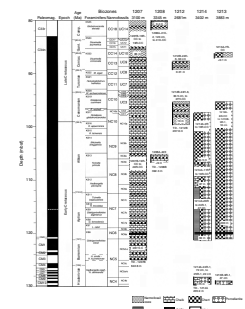
an earliest Berriasian age based on radiolarian and nannofossil assem-blages (H. Kano, pers. comm., 2005; Bown, this volume) and the sills themselves yield a mean $^{40}Ar$-$^{39}Ar$ incremental heating age of 144.6 ± 0.8 Ma (Mahoney et al., 2005). These data provide a constraint for the age of the origin of Shatsky Rise and a minimum estimate for the age of the Jurassic/Cretaceous boundary that is slightly older than recent esti-mates of ~141 Ma published by Bralower et al. (1990) and Pálfy et al. (2000) but consistent with the 145.5-Ma estimate of Gradstein et al. (2004). The new Jurassic/Cretaceous boundary age combined with mag-netism data (e.g., Nakanishi et al., 1999; Sager et al., 1999) suggest that the largest part of the rise was emplaced at rates between 1.2 and 4.6 km³/yr, rates similar to other large flood basalt provinces (Coffin and El-dholm, 1994; Sager, in press; Sager et al., this volume; Tominaga et al., this volume) (Fig. F10).

Various models have been proposed for LIPs including Shatsky Rise. These include a mantle plume model involving rapid eruption at a plume head tapering off to slower eruption at a plume tail (Sager and Han, 1993). A mantle plume model is supported by the fact that Shatsky Rise formed very rapidly at a triple junction of ocean ridges af-ter the triple junction had jumped 800 km (e.g., Nakanishi et al., 1999; Sager et al., 1999) and by the rapid rates of the initial emplacement fol-lowed by gradually diminishing volcanism. A second alternative, the "perisphere" model, involves a large asteroid impact on oceanic crust that excavates the underlying mantle, leading to eruption of an LIP (Rogers, 1982). This model has recently been proposed for Ontong Java Plateau (OJP) by Ingle and Coffin (2004) and Tejada et al. (2004). The two origin models should generate different sill geochemistry.

Nd-Pb-Sr isotope values of the sills exhibit a Pacific mid-ocean-ridge basalt (MORB) signature (Fig. F11) (Mahoney et al., 2005) that is consis-tent with a perisphere origin but not a plume-head origin, which would be associated with ocean island-like rather than MORB-like isotopic sig-natures. Although a contemporaneous impact to that which formed the >70-km-diameter Morokweng crater in South Africa dated at 144.7 ± 1.9 and 146.2 ± 1.5 Ma (Koeberl et al., 1997) may have led to the formation of Shatsky Rise, such an impact would have caused massive disruption of the seafloor that is not observed on seismic lines near the Southern High. Moreover, an impact would have caused near-instantaneous LIP formation, which is clearly not the case for Shatsky Rise. A third, com-promise model is that a large impact (i.e., Morokweng) may have strengthened existing mantle plumes on the other side of Earth from the impact site (Abbott and Isley, 2002), but once again this scenario would not produce a MORB basement signature.

An alternative to the perisphere and plume models is that the ridge jump that occurred around the time that Shatsky Rise formed led to a change in the stress regime (i.e., decompression), which promoted melting of anomalously warm lithosphere (Sager, in press). This alterna-tive would explain the MORB geochemical signature and avoid poten-tial difficult explanations of the coincidence of the ridge jump and either mantle plume activity or impact. However, the notion that de-compression could cause such significant melting is untested. Clearly, additional basement sampling and model testing are required to resolve the origin of Shatsky Rise.

F6. Stratigraphic summary for 85–60 Ma, p. 31.
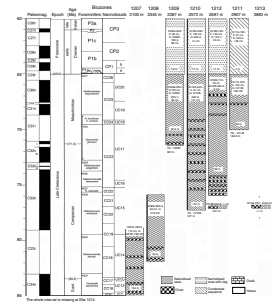


F7. Stratigraphic summary for 65–40 Ma, p. 32.
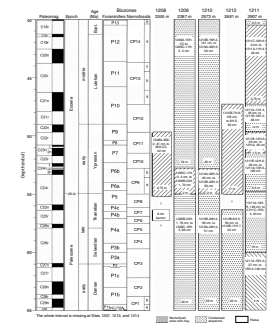


F8. Stratigraphic summary for 45–20 Ma, p. 33.
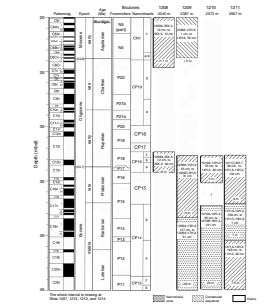


F9. Stratigraphic summary for 25–0 Ma, p. 34.
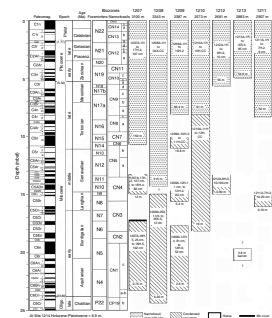
## Cretaceous Oceanic Anoxic Events: Production of Highly Organic Rich Horizons

Greenhouse climate conditions in the mid-Cretaceous led to a transformation of marine environments that caused rapid turnover of ecosystems and profound changes in biogeochemical cycles. One of the most remarkable consequences of the changes in climate and ocean circulation was the widespread deposition of organic carbon ($C_{org}$)-rich sediments, also known as "black shales," during OAEs (Schlanger and Jenkyns, 1976; Jenkyns, 1980; Sliter, 1989; Arthur et al., 1988; Bralower et al., 1993; Erbacher and Thurow, 1997; Wilson and Norris, 2001; Leckie et al., 2002). Although the ultimate trigger(s) of OAEs remain elusive, there is growing evidence for a link with massive volcanism associated with the emplacement of LIPs (e.g., Vogt, 1989; Larson, 1991; Sinton and Duncan, 1997; Larson and Erba, 1999; Snow et al., 2005). Thus, one of the goals of Shatsky Rise drilling was to determine the record of OAEs in the northwest Pacific and their stratigraphic relationship with increasingly well constrained ages for LIPs.

Highly carbonaceous sedimentary rocks that correlate to early Aptian OAE1a were recovered at Sites 1207 and 1213 (Fig. F12). At Site 1207, OAE1a is found within 45 cm of finely laminated, dark brown radiolarian claystone. Organic carbon contents in these horizons (up to 35 wt%) are among the highest values measured from OAEs and are similar to values measured in contemporaneous units from other Pacific deepsea sites (e.g., Baudin et al., 1995; Jenkyns, 1995). A detailed analysis of carbon isotopes measured on the organic fraction of the sediments at Site 1207 (Dumitrescu and Brassell, submitted [N1]) allows precise correlation to detailed features in curves from other sections (e.g., Menegatti et al., 1998). These data demonstrate that the lower part of OAE1a was not recovered at Site 1207 but the upper part of the event is relatively complete.

The Site 1213 $C_{org}$-rich units include clayey porcellanites and radiolarian porcellanites with associated minor tuff containing $C_{org}$ as high as 25 wt%. At Site 1214, a black laminated claystone unit contains a distinctive radiolarian assemblage that suggests the recovered sediments correlate to the OAE1a interval (e.g., Erbacher and Thurow, 1997), but low $C_{org}$ contents (<1.4 wt%) indicate the peak of the event was not recovered (Bralower, Premoli Silva, Malone, et al., 2002).

Sedimentology of the lower Aptian interval from Sites 1207, 1213, and 1214 was studied in detail by Marsaglia (this volume). She attributed a pulse of ash input just below the $C_{org}$-rich horizon to the same volcanic event that caused the emplacement of OJP at this time, although the ash probably did not originate on OJP or Shatsky Rise. Volcanic material in the organic-rich horizon suggests that it cooled and altered in subaerial environments, indicating the presence of nearby emergent volcanoes. Intervals of organic-rich sediments are finely laminated and alternate with slightly bioturbated sediments, indicating alternating anoxia and oxygenated conditions. The close association of organic-rich and volcanic rocks provides additional evidence of a temporal relationship, but not necessarily a direct causal link, between anoxia and volcanism.

$C_{org}$ contents of lower Aptian intervals from Sites 1207 and 1213 (up to 35 wt%) are the highest levels recorded for OAE1a and are among the highest recorded for any OAE. These levels attest to extraordinary environmental conditions during OAE1a. Rock-Eval and gas chromatogra-

**F10.** Magnetic polarity interpretation of Lower Cretaceous sediments, p. 35.
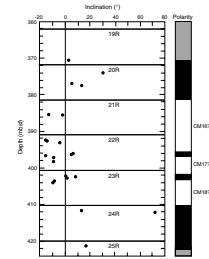
**F11.** Geochemistry of diabase sills, p. 36.
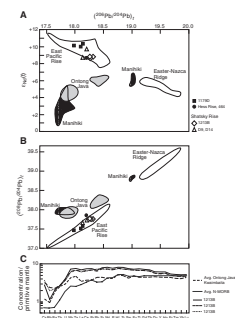
**F12.** Carbonate, $C_{org}$, and hydrogen index for lower Aptian sedimentary rocks, p. 37.
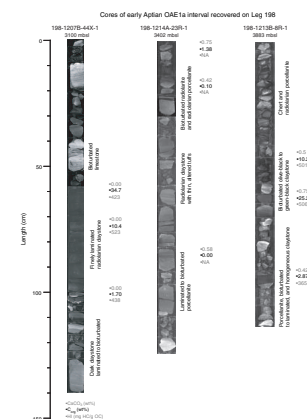
phy–mass spectrometry (GC-MS) analyses of extractable hydrocarbons and ketones indicate that the organic matter in the $C_{org}$-rich units is almost exclusively algal and bacterial in origin. GC-MS data show biomarkers associated with cyanobacteria. The prevalence and character of bacterial biomarkers suggest the existence of microbial mats at the time of deposition (Dumitrescu and Brassell, 2005). Compounds identified in Leg 198 sediments also include the oldest known alkenones, a characteristic biomarker of haptophyte algae (Brassell et al., 2004), extending the geologic record of these compounds by 15 m.y. The high $C_{org}$ content and its nearly pristine nature suggest highly favorable depositional conditions including high primary productivity, anoxic deepwater environments, and subsequent shallow burial. Organic geochemical data indicate that profound changes in prokaryote and protistan populations were involved in sequestration of $C_{org}$ during OAE1a (Dumitrescu and Brassell, 2005).

Recovery of mid-Cretaceous sediments at all of the Leg 198 sites was hampered significantly by the presence of widely disseminated chert (e.g., **Fontilea et al.,** this volume). In the poorly recovered intervals, geophysical logs integrated with sedimentological, biostratigraphic, and physical property data are critical to interpreting depositional history. The geophysical logs confirm the presence of a signal from OAE1b even though no organic-rich sediments were recovered in this interval (Fig. **F13**) (Robinson et al., 2004). This is significant because OAE1a and OAE1b are thought to have had extremely widespread or global extents, whereas the other Albian events (OAE1c and OAE1d) are more regional (Bralower et al., 1993; Erbacher and Thurow, 1997; Leckie et al., 2002). It is therefore surprising that OAE2 at the Cenomanian/Turonian boundary, an event widely regarded as global in extent (e.g., Schlanger et al., 1987), does not appear to be present in the logs. This interval is either unconformable or highly condensed on Shatsky Rise. Geophysical logs suggest that lower Aptian and lower Albian carbonates are relatively lithified compared to surrounding sediments, likely a result of increased siliceous cementation (Robinson et al., 2004). Increased biosiliceous production during OAEs in the early Aptian (OAE1a) and early Albian (OAE1b) suggest widespread increased productivity and delivery of biolimiting nutrients from hydrothermal sources.

## Late Cretaceous and Paleogene Deepwater Circulation: Identifying Switches in Source Regions

One of the major objectives of drilling the Leg 198 depth transect was to establish deepwater circulation patterns for the Late Cretaceous and Paleogene and elucidate changes over long timescales (millions of years) along with those that took place abruptly in a geologic sense (thousands of years). Drilling recovered a number of abrupt events as well as a nearly complete Campanian–Oligocene section at sites from a range of water depths (Bralower, Premoli Silva, Malone, et al., 2002; 2002). These events and the long-term section have been the subject of a host of investigations aimed at unraveling changes in deepwater circulation patterns. A number of techniques including stable isotopes, neodymium isotopes, trace elements, and micropaleontology have been used to pursue these objectives. The predominant ooze and chalk lithology at relatively shallow burial depths contains moderately well preserved foraminifers throughout that are suitable for detailed stable isotope and other geochemical investigations.

**F13.** Correlation of the Hauterivian–Albian between Sites 1207 and 1213, p. 38.
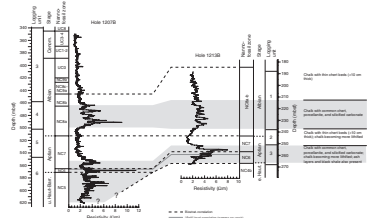
Frank et al. (2005) applied stable and neodymium isotope studies to reconstruct Pacific deepwater circulation patterns in the Maastrichtian. These data suggest that during the early Maastrichtian the source regions for deep waters at the paleodepths of Shatsky Rise (strictly speaking, intermediate waters) changed from the northern Pacific to the Southern Ocean. An abrupt warming event in the mid-Maastrichtian at ~69 Ma that led to the extinction of inoceramid clams is associated with changes in benthic foraminiferal isotopic values. This mid-Maastrichtian event (MME) was recovered at three sites on Shatsky Rise and is graphically represented in cores by the abrupt appearance and disappearance of abundant inoceramid shells and prisms (Bralower et al., 2002). The MME has previously been interpreted in terms of changing deepwater source regions (MacLeod and Huber, 1996; MacLeod et al., 1996). Data from Shatsky Rise cores reveal a sudden 2°–3°C intermediate water warming, consistent with a switch to a low-latitude source region (Fig. F14) (Frank et al., 2005). Neodymium isotope analyses show abrupt excursions during the MME, also indicating a different intermediate water source. Together, neodymium and benthic isotope data suggest a temporary Tethyan Sea source for intermediate waters. Tethys has been proposed as the source of intermediate and deep waters in other warm intervals including the mid-Cretaceous (e.g., Brass et al., 1982), PETM (e.g., Kennett and Stott, 1991), and early Eocene (Scher and Martin, 2004) but has not previously been implicated for the MME.

Planktonic foraminiferal oxygen isotope values indicate that the MME is characterized by an abrupt rise (~2°–3°C) in sea-surface temperatures (SSTs). Increased productivity during the event is suggested by a collapse in the surface water $\delta^{13}C$ gradient (Fig. F14) (Frank et al., 2005). Changes in planktonic and benthic foraminiferal assemblages also suggest higher productivity. Leg 198 data show for the first time a clear surface water perturbation during the MME. Although the exact details remain to be elucidated, the significant surface water response during the MME suggests that the ultimate origin of the event was climatic and that changes in surface water oceanography were responsible for modified intermediate water circulation and, ultimately, for the inoceramid extinctions.

Dutton et al. (2005) investigated long-term changes in surface and deepwater properties and circulation patterns using a combination of $\delta^{18}O$ measurements of planktonic foraminifers and coupled $\delta^{18}O$ and Mg/Ca analyses of benthic foraminifers (Fig. F15). Interpretation of Mg/Ca values helps determine how much of the $\delta^{18}O$ change is associated with temperature and how much with variation in the isotopic composition of seawater due to fluctuation in local or regional salinity or in ice volume.

SST trends are similar to those proposed for other Paleogene sections such as Site 577 on Shatsky Rise (e.g., Corfield and Cartlidge, 1991) and Site 865 on Allison Guyot (Mid-Pacific Mountains) (Bralower et al., 1995). Stable SSTs of ~22°C are proposed for the Paleocene and early Eocene. Considerable intersample variability during this interval is used as evidence for significant seasonality, whereas the lower–middle Eocene interval shows less variability and is interpreted to have been characterized by less seasonality. SSTs began to decrease in the late early Eocene and reached 17°C in the middle Eocene. Intermediate water temperatures determined from benthic $\delta^{18}O$ values remained steady at 9°–11°C in the Paleocene but increased to 13°C in the latest Paleocene and early Eocene. Cooling of intermediate waters began in the middle Eocene and temperatures decreased to 3.5°C by the late Eocene (Fig.

**F14.** Carbon, oxygen, and neodymium isotope records, p. 39.
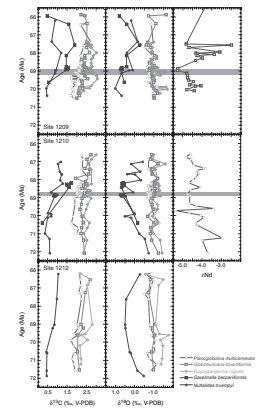
**F15.** Paleogene stable isotope results, p. 40.
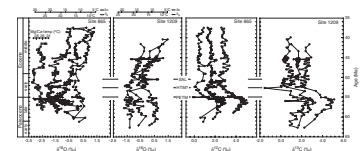
F15). Benthic foraminiferal Mg/Ca values help constrain the proportion of the $\delta^{18}O$ change that can be attributed to temperature change and to changes in the isotopic composition of seawater as a result of Antarctic glaciation. These data suggest intensification of glaciation in the middle Eocene with accumulation of continental ice sheets of up to ~50% of modern volume.

Stable isotope data reveal interesting changes in surface-thermocline and thermocline-deepwater gradients. Notably, there is a collapse in the gradient between thermocline and deepwater $\delta^{18}O$ values in the early Eocene (52 Ma) at the peak of the Early Eocene Climatic Optimum (EECO) and at the time when seasonality decreases abruptly. Dutton et al. (2005) proposed that the decreased gradient preconditioned the water column for a brief switch in intermediate water circulation. This interval is marked by one sample with an extremely negative benthic $\delta^{13}C$ value and increased $\delta^{18}O$ values of planktonic and benthic foraminifers that is tentatively correlated to the "Chron 24n" event, also known informally as the "ELMO" event (53 Ma) at Walvis Ridge (Zachos, Kroon, Blum, et al., 2004; Lourens et al., 2005). Dutton et al. (2005) speculated that the event was associated with a transient low-latitude, saline intermediate water source.

Neodymium isotope measurements of fish teeth provide an independent means of tracking Late Cretaceous and Paleogene intermediate and deepwater circulation patterns (Fig. F16) (Thomas, 2004, 2005). Site 1209 and 1211 Nd isotope data contain evidence for two end-member sources of deep waters: the Southern Ocean and the North Pacific Ocean. Data from both sites suggest a gradual change in the dominant source of deep waters on Shatsky Rise in the latest Cretaceous from the Southern Ocean to the North Pacific. North Pacific waters continued to bathe Shatsky Rise through the EECO, the time of warmest deep-sea conditions during the Cenozoic. Thomas (2004) proposed that climate change altered precipitation patterns in source regions of the Southern Ocean and North Pacific Ocean, rendering the latter waters denser than the former. These data demonstrate a 20-m.y. interval of fundamentally different circulation from that of the modern day (Fig. F16). As global deep waters continued to cool starting in the middle Eocene, the source of deep waters shifted back to the Southern Ocean. Deepwater properties changed fundamentally in the Eocene/Oligocene boundary interval, which demonstrates a significant lithologic transition at the Shatsky Rise sites (Bralower, Premoli Silva, Malone, et al., 2002; Averyt et al., this volume).

## New Interpretations for Extinction Events at the Cretaceous/Tertiary Boundary

The origin of extinctions at the Cretaceous/Tertiary (K/T) boundary (65 Ma) is well understood; however, the effect of the event on marine ecosystems is not well constrained. A remarkable set of cores was taken across the K/T boundary on the Southern High at Sites 1209, 1210, 1211, and 1212 (Fig. F17) that has promoted studies aimed at addressing these issues.

The K/T boundary succession is similar at all of these sites (Fig. F17). The boundary lies between uppermost Maastrichtian (nannofossil Zone CC26) white to very pale orange slightly indurated nannofossil ooze and an 8- to 12-cm-thick layer of basal Paleocene (foraminiferal Zone Pa) grayish orange foraminiferal ooze. The substantial thickness of the

F16. Paleogene neodymium isotope records, p. 41.
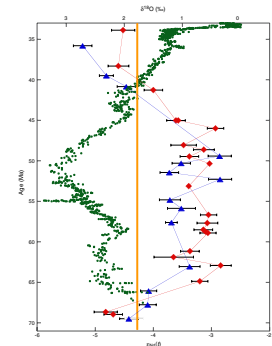
F17. K/T boundary sections on Shatsky Rise, p. 42.
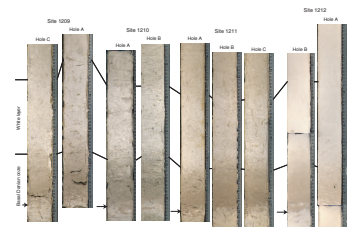
uppermost Maastrichtian *Micula prinsii* (CC26) Zone and the lowermost Danian *Parvularugoglobigerina eugubina* (Pα) Zone indicates that the K/T boundary is relatively expanded on the Southern High of Shatsky Rise compared to other deep-sea sites. The Leg 198 sections represent some of the best preserved and least disrupted deep-sea records of the K/T extinction event and subsequent biotic radiation.

The boundary between the uppermost Maastrichtian and the lowermost Paleocene is clearly bioturbated, with an irregular surface contact and pale orange burrows extending 10 cm into the white Maastrichtian ooze. The deepest sections of these burrows yielded highly abundant, minute (<75 μm), planktonic foraminiferal assemblages dominated by triserial *Guembelitria* with rare *Hedbergella holmdelensis* and *Hedbergella monmouthensis*, which suggest the presence of the lowermost Paleocene Zone P0.

In the uppermost Maastrichtian (*Abathomphalus mayaroensis* Zone), faunal preservation is variable from layer to layer, ranging from fair to progressively poorer approaching the top of the Cretaceous: faunas become chalky in aspect and tend to dissolve and specimens are highly fragmented, in contrast to the excellent preservation of the minute assemblages of Zone P0 recovered in the deepest part of the burrows (**Premoli Silva et al.,** this volume). Similar good preservation characterizes the still minute *Guembelitria*-dominated assemblage, containing very rare, minute five-chambered *P. eugubina* at the top of the burrows and in the millimeter-thick depressions on the irregular surface of the uppermost Maastrichtian white ooze. One centimeter above the lithologic change, planktonic foraminifers start to diversify, acquiring abundant biserial heterohelicids and very subordinate trochospiral taxa (*Eoglobigerina*, *Globoconusa*, and still rare *P. eugubina*). Planktonic foraminiferal assemblages of Zone Pα = total range of *P. eugubina*), still dominated by triserial *Guembelitria* and biserial chiloguembelinids and woodringinids, also contain common larger-sized hedbergellids that disappear some 20 cm above the base of the zone. Such a range of hedbergellids is anomalously higher than that known in the literature (i.e., Keller, 1988; Olsson et al., 1999) and may be an artifact resulting from either reworking or sampling procedure. Quantitative analysis shows that *Guembelitria* displays an opposite trend with respect to both biserial heterohelicids and *P. eugubina*. Moreover, at Shatsky Rise biserial and triserial heterohelicids continue to dominate the assemblages well within Zone P1, and only ~1.5 m above the lithologic change (233.45 meters below sea floor [mbsf]) trochospiral taxa make up 25% of the assemblage concomitantly with the near total absence of triserial *Guembelitria*.

High-resolution nannofossil assemblage studies across the boundary at Site 1210 by Bown (2005) demonstrate that 10 Late Cretaceous species survived the K/T boundary extinction, including two species previously thought to have gone extinct (Fig. F18). Although it is well established that ~93% of species went extinct at the boundary, we have a poor understanding of the ecological preferences of the taxa that survived and whether these preferences differed from those of species that went extinct. Bown (2005) proposed that the extinctions were highly selective and related to trophic strategy and habitat preference. Survivors include neritic taxa that are adapted to unstable environments, whereas the species that went extinct were largely open-ocean taxa that have lower tolerance to environmental stress. Some survivors also may have possessed a cyst stage that allowed them to temporarily escape from hostile surface water conditions.

**F18.** K/T survivor and incoming Cenozoic nannofossils, p. 43.
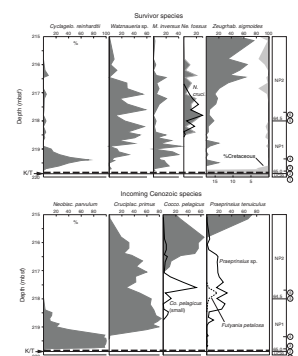
## Paleocene/Eocene Thermal Maximum on Shatsky Rise: Biotic, Climatic, and Oceanographic Signatures

The PETM (55 Ma) was a profound yet transient (~120–200 k.y.) warming event with a geologically abrupt onset (several thousand years). A number of different causal mechanisms have been proposed for the event, all of which involve input of a massive amount of greenhouse gas into the ocean-atmosphere system (e.g., Dickens et al., 1995; Kent et al., 2003; Svensen et al., 2004). The magnitude and rate of environmental change during this event led to transformation of marine and terrestrial communities (e.g., Hooker, 1996; Kelly et al., 1998; Crouch et al., 2001; Bralower, 2002), including the most severe deep-sea extinction event in the last 90 m.y. (e.g., Thomas, 1990, 1998) and significant shifts in continental weathering patterns and marine geochemical cycling (Gibson et al., 1993; Ravizza et al., 2001).

The PETM has intrigued paleontologists and paleoceanographers because the event serves as a worst-case scenario for modern global warming and its effect on ocean circulation and its implication for biotas (e.g., Bains et al., 1999; Norris and Röhl, 1999). However, the lack of high-quality tropical records has prevented a thorough understanding of the physics of the event. Oxygen isotope data from high-latitude sites indicate SST increases of as much as 10°C, and data from a range of latitudes suggest that bottom water temperatures increased by 5°C (Kennett and Stott, 1991; Bralower et al., 1995). One of several existing quandaries in the interpretation of the PETM is the lack of a clear signal for warming at tropical latitudes. The event has been attributed to a rapid rise in greenhouse gas levels that should lead to warming at all latitudes (e.g., Huber and Sloan, 1999; Bice and Marotzke, 2001). A number of tropical records, including ODP Sites 999 and 1001 from the Caribbean Sea and Site 1051 from Blake Nose (western North Atlantic Ocean), are deeply buried and are thus unsuitable for foraminiferal stable isotope analyses. Existing shallow sections, including DSDP Site 577 on Shatsky Rise and ODP Site 865 from Allison Guyot, are stratigraphically incomplete (e.g., Pak and Miller, 1992; Bralower et al., 1995).

The PETM interval was cored in nine holes at Sites 1209, 1210, 1211, and 1212 on the Southern High and Site 1208 on the Central High (Fig. F19). At the Southern High sites, the PETM is stratigraphically complete and corresponds to an 8- to 23-cm-thick layer of yellowish brown clayey nannofossil ooze with a sharp base and a gradational upper contact. These sediments have been the subject of a host of geochemical and paleontological investigations.

Combined measurements of oxygen isotopes and Mg/Ca ratios from the same planktonic foraminifers from Site 1209 imply a 4.5°–5.0°C increase in tropical Pacific SSTs during the PETM (Fig. F20) (Zachos et al., 2003), the first definitive evidence for warming in the tropics during the event. Mg/Ca ratios indicate that the oxygen isotope signal is affected by a substantial change in sea-surface salinity (SSS). The warming trends at Site 1209 combined with those from high-latitude sites are consistent with a two- to threefold increase in atmospheric $pCO_2$ over background levels.

The PETM environmental change caused dramatic turnover in planktonic marine faunas and floras. One of the dominant nannolith genera, *Fasciculithus,* was replaced by *Zygrhablithus bijugatus*, a holococcolith species that is often a highly abundant component of Eocene assemblages. The genus *Discoaster* is highly abundant, likely as a result of warming or increased oligotrophy (Bralower, 2002). Planktonic fora-

**F19.** PETM sections on Shatsky Rise, p. 44.
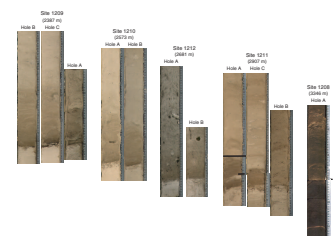


**F20.** Stable isotopes and trace elements from the PETM, p. 45.
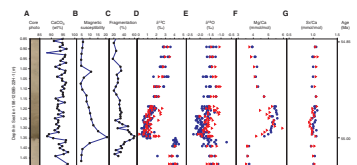
miniferal assemblages contain an ephemeral group of ecophenotypes or short-lived species of the genera *Acarinina* and *Morozovella* (Kelly et al., 1996). Gibbs et al. (2006) investigated nannofossil assemblage changes at Site 1209 in detail. They observed a prominent increase in species of *Biantholithus, Markalius, Braarudosphaera,* and *Thoracosphaera* at the base of the event, followed by an increase in *Z. bijugatus* and species of *Discoaster* and *Sphenolithus* some 10 cm above the event base (Fig. F21). The former genera are well-established disaster taxa that thrived in stressful environments in the immediate aftermath of the Cretaceous/ Tertiary boundary event (e.g., Thierstein and Okada, 1979; Pospichal, 1996; Bown, 2005). The latter taxa are known to prefer warm and oligotrophic surface water conditions (e.g., Aubry, 1998; Bralower, 2002). Although there are a number of possible explanations for the peaks in abundance of the disaster taxa, the preferred explanation is extremely oligotrophic conditions resulting from an increasingly stratified water column (Gibbs et al., 2006).

The PETM coincides with the most significant benthic foraminiferal extinction event of the last 90 m.y. (Tjalsma and Lohmann, 1983; Thomas, 1990). A great deal of attention has been devoted to understanding the detailed assemblage changes and elucidating the selectivity of the extinction. For example, the extinction was exclusive to epifaunal rather than infaunal taxa and shelf taxa appear to have been much less affected than those in the deep sea (e.g., Thomas and Shackleton, 1996; Thomas, 1998; Spiejer and Schmitz, 1998). A significant question—the cause of the extinction—remains largely unanswered. The timing and pattern of the extinction are remarkably similar between sites, and this is hard to explain using most viable extinction mechanisms (e.g., Thomas, 2003). High-resolution studies of benthic foraminiferal assemblages from the Leg 198 PETM sections show that the onset of the event was characterized by extinction of ~30% of species and a low-diversity assemblage dominated by dwarfed specimens of *Bolivina advena* (Kahio et al., submitted [N2]). This assemblage persisted for ~30 k.y. and was followed by a shift to an assemblage dominated by dwarfed specimens of *Quadrimorphina profunda* that lasted for 55 k.y. The low diversity and small size of the assemblage are possibly a result of lower deepwater oxygen conditions that resulted from PETM warming. At the same time as benthic foraminiferal size decreased, the size of surface water planktonic taxa increased significantly, possibly in response to increased thermal stratification and decreased nutrient supply (Kahio et al., submitted [N2]).

The depth transect of sections can be used to elucidate the response of the lysocline and calcite compensation depth (CCD) during the PETM. Input of a massive amount of greenhouse gas (i.e., $CO_2$ or $CH_4$) at the onset of the event should result in rapid shoaling of the lysocline and CCD (e.g., Dickens et al., 1997; Dickens, 2000). The Shatsky Rise PETM sections show clear evidence for lysocline shoaling including an abrupt change in the nature of sediments from nannofossil ooze to clay-rich nannofossil ooze and a rapid decrease in $CaCO_3$ content. Detailed investigation of PETM sediments by **Colosimo et al.** (this volume) shows a sharp increase in foraminiferal fragmentation at the base of the event corresponding to deterioration in visual preservation. Comparison of sites suggests a minimum lysocline shoaling of ~500 m in the tropical Pacific Ocean during the PETM. The sites also show evidence of $CaCO_3$ dissolution within the sediment column, carbonate "burn down," a predicted response to a rapid change in deepwater satu-

**F21.** Nannofossil diversity and abundance for the PETM, p. 46.
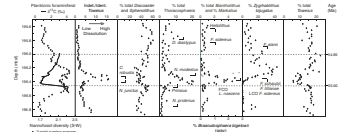
ration (Walker and Kasting, 1992). The magnitude of this shoaling is far less than that in the Atlantic Ocean (e.g., Zachos et al., 2005), suggesting that a substantial amount of greenhouse gas was mixed via the deep ocean and that circulation patterns were broadly similar to those of the present day.

## Abrupt Warming Events: "Hyperthermals" in the Paleogene

The PETM is recognized as the most significant short-term warming event. However, the event may not be unique and a number of other intervals of rapid temperature increase, although smaller in magnitude, may also exist in the warm early Paleogene (Thomas et al., 2000; Bralower et al., 2002). One of these so-called "hyperthermals" in the early late Paleocene at ~58.4 Ma corresponds to a prominent clay-rich ooze at Sites 1209, 1210, 1211, and 1212 (**Hancock and Dickens,** this volume) and may have had evolutionary significance. The clay-rich layer contains common crystals of phillipsite, fish teeth, and phosphatic micronodules. This event coincides with the evolutionary first occurrences of the nannoplankton *Heliolithus kleinpellii* and primitive discoasters. *H. kleinpellii* is an important late Paleocene zonal marker; the discoasters are dominant components of tropical and subtropical assemblages for most of the remainder of the Cenozoic. Planktonic foraminifers in the clay-rich layer are characterized by a low-diversity, largely dissolved assemblage dominated by the genus *Igorina*. Two species of *Igorina*, *I. pusilla* and *I. tadjikistanensis,* dominate samples (**Petrizzo,** this volume).

The abundance of phillipsite and fish teeth suggests pervasive dissolution of carbonate resulting from prolonged seafloor exposure or at least very slow sedimentation. A critical question remains as to whether the foraminiferal assemblages that are clearly altered by dissolution also reflect a significant perturbation in surface waters. Although **Petrizzo** (this volume) concluded that the foraminiferal assemblage shifts result primarily from dissolution, nannofossil assemblages (T. Bralower, unpubl. data) suggest that the event corresponds to an abrupt surface water warming. Clearly, more research is required to answer this question. Nevertheless, it is of note that the early late Paleocene "hyperthermal" event was also recovered on Walvis Ridge in the South Atlantic Ocean and this interval is characterized by similar lithologic composition and planktonic foraminiferal assemblages to the contemporaneous interval on Shatsky Rise (Zachos, Kroon, Blum, et al., 2004).

Magnetic susceptibility records from the Southern High transect show a strong orbital cyclicity dominated by eccentricity (100- and 400-k.y. frequencies) (**Westerhold and Röhl,** this volume). The early late Paleocene event corresponds to an eccentricity minimum, suggesting that it is a response to an orbital change in climate. Other susceptibility minima also correspond to horizons characterized by increases in clay content, some of which also contain phillipsite and fish debris. These events may also turn out to be hyperthermals. The cycles appear to be controlled by variations in the amount of dissolution as indicated by variations in foraminiferal fragmentation and benthic/planktonic foraminiferal ratios (**Hancock and Dickens,** this volume). Moreover, **Hancock and Dickens** (this volume) found an increase in the amount of dissolution between 45 and 33.7 Ma at Sites 1209 and 1211.

## Neogene

The Neogene–Holocene succession was recovered at seven sites drilled on Shatsky Rise along a latitudinal transect that spans ~6° of latitude from 37°N on the Northern High to 31°N on the Southern High. The most expanded section, which spans the interval from the upper middle Miocene to the Holocene and has a sedimentation rate as high as 42 m/m.y., was recovered at Site 1208 on the Central High. A similar section with a lower sedimentation rate (28 m/m.y.) was recovered at Site 1207 on the Northern High. Sedimentation rates at Southern High sites (Sites 1209–1213) are <14 m/m.y., at least partially as a result of the lower production of biosiliceous and carbonate materials. Moreover, the Central and Northern High sites appear to have received a large supply of fine sediment from bottom water currents and eolian transport. The upper Miocene and younger sections at all Leg 198 sites rests unconformably on middle Miocene sediments. The middle Miocene and most of the lower Miocene are represented by incomplete, highly condensed sequences that are dark in color, enriched in clay content, and may be capped by manganese crusts. These unconformities from the lower to middle Miocene and the lower Miocene to lower Oligocene are partially equivalent from site to site and suggest that regional oceanographic processes controlling erosion and dissolution had a major affect on sedimentation.

Today, Shatsky Rise lies in a subtropical water mass toward the north end of the range of the warm-water Kuroshio Extension Current. North of the Northern High lies a significant front, a transition region between subtropical and subarctic water masses. The transition zone waters are derived from off the coast of northern Japan, where the cold, nutrient-rich Oyashio Current mixes with the warm, nutrient-poor Kuroshio Current. Even though at 10 Ma in the late Miocene the Northern High was located father south at ~32°N paleolatitude (R. Larson, pers. comm., 2001), because of its proximity to the transition zone the northern part of Shatsky Rise was a location highly sensitive to past climatic variations.

Significant oceanographic changes occurred during the Neogene that had profound effects on circulation and distribution of water masses in the Pacific Ocean; these changes appear to be reflected in the sedimentary record recovered at Shatsky Rise. An event at 14.5 Ma has been associated with the formation of the East Antarctica Ice Sheet (Kennett et al., 1985); another event at 11 Ma is related to closure of the Indo-Pacific Seaway (Romine and Lombari, 1985). These events led to a steepening of temperature gradients and intensification of North Pacific gyral circulation including the ancestral Kuroshio Current. The modified circulation resulted in development of a distinct North Pacific transitional water mass, separated from the northern subpolar region, and northward displacement of temperate organisms. Moreover, these events may be responsible for hiatuses and/or condensed intervals of variable duration that characterize sediment deposition throughout the rise during the late early and middle Miocene.

The decrease in carbonate content at the shallowest Site 1209 on the Southern High in the middle Miocene is accompanied by the presence of several more clay rich intervals (Malone, this volume). This pattern is similar to those observed at the deeper Sites 1207 and 1208. Based on biostratigraphic data, these clay horizons are condensed intervals, most likely produced by dissolution of carbonate at the seafloor during the middle and late early Miocene. Such a phenomenon would be consis-

tent with the reported shoaling of the global lysocline and CCD through the early and middle Miocene (Rea and Leinen, 1985). Studies of previously drilled sites suggest that the lysocline was as shallow as 3 km during the early Miocene. Leg 198 data indicate that the lysocline might have been even shallower (<2.4 km) during much of this period. The alternating carbonate- and clay-rich lithologies suggest that the process(es) responsible for slow sedimentation was somewhat cyclic, perhaps related to fluctuating CCD levels (discussed above) and/or intensity of erosional currents.

Northward migration of Shatsky Rise by 5° latitude since the late Miocene (R. Larson, pers. comm., 2001) is accompanied by changes in biogenic components of the sediments as well as their state of preservation. Although the middle Miocene record displays slightly different ages from site to site, calcareous plankton assemblages are rather uniform and diverse across Shatsky Rise and display warm, subtropical affinities. Since the late Miocene, however, a faunal and floral gradient has been established across Shatsky Rise. Calcareous plankton assemblages progressively lose the warmest taxa from southern to northern sites, including discoasters and sphenoliths among calcareous nannofossils and *Globigerinoides* and keeled globorotaliids among planktonic foraminifers. The resulting marked decrease in diversity is reflected in assemblages that assume temperate (occasionally cold-temperate) affinities at the more northern Sites 1207 and 1208. The changes in calcareous plankton assemblages are paralleled by a progressive decrease in preservation. Over the same interval, diatoms become progressively more abundant toward the north. Based on magnetostratigraphic age constraints (see **Evans et al.,** this volume), the first occurrence of biosiliceous organisms at Shatsky Rise is dated at ~12 Ma in the late middle Miocene at Sites 1207 and 1208 but at ~6.5 Ma in the latest Miocene at Site 1209 or ~5 Ma in the earliest Pliocene at Site 1210 on the Southern High.

Diatoms increase markedly in abundance at ~8 Ma, just after a change in Pacific Ocean circulation associated with the closure of the Indonesian Seaway that caused intensification of North Pacific gyral circulation (Kennett et al., 1985); a strengthened west wind drift likely increased upwelling along this boundary and created a more well-established North Pacific transitional water mass separated from the northern subpolar region. The amount of diatoms observed in the sediments is variable from layer to layer, probably as a function of the degree of carbonate dissolution. However, peaks in abundance of biosiliceous material occur in the latest Miocene, late early Pliocene, and late Pliocene. Based on magnetostratigraphic age models (**Evans et al.,** this volume), the highest abundance of biosiliceous material across Shatsky Rise was recorded between ~3.2 and 2.6 Ma. A significant peak in opal accumulation rates also occurs between 3.2 and 2.75 Ma at other sites from the northern Pacific (Haug et al., 1995; Maslin et al., 1995). The origin of this peak and subsequent decline is uncertain, but the base of this peak corresponds to the beginning of long-term global cooling, which culminated in Northern Hemisphere glaciation, and the top of the peak corresponds to the rapid advance of Northern Hemisphere glaciers.

Regional studies (e.g., Natland, 1993) of ash distribution across Shatsky Rise suggest that ash beds present in the last 2.6 m.y. at Site 1208 are wind-borne sediments that likely were carried to the site from volcanic eruptions along the Japan and/or Kurile magmatic arc systems. The maximum and subsequent waning of ash input expressed in the

frequency of ash beds (see Gadley and Marsaglia, this volume) could be linked to changes in volcanic activity along the arc systems or to changes in wind patterns over time. Isolated pumice clasts were most likely rafted to the site by the Kuroshio Current, which passes across the submerged pumice-producing calderas of the Izu-Bonin magmatic arc to the west (see Taylor, Fujioka, et al., 1990) and flows directly over Shatsky Rise.

Changes in the geographic distribution of water masses through time also affected other fossil groups. In particular, Neogene planktonic foraminifers show distinct stratigraphic changes between assemblages dominated by subtropical and tropical taxa and those dominated by taxa with cool, temperate affinities. Moreover, faunas at Site 1208 are considerably richer in warmer, tropical taxa than those at Site 1207, which is located only ~1° to the north. This suggests that for much of the Neogene, Sites 1207 and 1208 were located in a region with sharp temperature gradients.

The Pliocene–Pleistocene at Site 1207 on the Northern High is particularly rich in siliceous microfossils, most likely due to cool, productive waters, which were also responsible for the paucity of tropical–subtropical species of planktonic foraminifers at this location. The influx of warmer-water planktonic foraminifers and reduction of biosiliceous plankton to the south at Sites 1209 to 1213 show the paleobiogeographic and paleoceanographic importance of the Shatsky Rise drill sites near the path of the Kuroshio Current.

One of the most significant features of the upper Miocene through Pleistocene sections recovered at Shatsky Rise is the decimeter- to meter-scale cycles between darker and lighter horizons. The darker-colored intervals in general contain higher amounts of very well preserved biosiliceous material, whereas calcareous plankton assemblages have suffered a greater amount of dissolution and are of cold-water nature. Calcareous plankton preservation is considerably better in the light-colored layers that have fewer diatoms. The darker layers are interpreted as probably representing intervals of higher surface water productivity as well as periods of higher carbonate dissolution. This interpretation is supported not only by the richness in diatoms in the darker layers but also by the abundance of some planktonic foraminifers such as *Globigerina bulloides*, a taxon that typifies the subpolar bioprovince and/or proliferates in upwelling regimes. Based on average sedimentation rates of 18.4 m/m.y. over the last 8 m.y. at Site 1207, the cycle frequency appears to be similar to that of glacial–interglacial cycles, with the darker beds representing glacials and the lighter beds representing interglacials. It is worth mentioning that prior to the onset of cyclic patterns at 8 Ma, calcareous plankton were definitely warmer in character than in the Pliocene–Pleistocene.

The ~5° of latitude that separates the Northern High drill site from those drilled on the Southern High is such a distance that one can expect significant change in oceanographic regime especially during unstable climatic conditions at the various sites. The most distinct cycles in terms of color variation and other physical properties occur in the upper Neogene. These are best represented by the total color reflectance (L*) records from Sites 1207–1209. The Pleistocene–Holocene color data at these sites exhibit the "classic" asymmetric glacial–interglacial cycle pattern. The transitions are mostly gradational, although several glacial/interglacial contacts are sharp. Interglacials are characterized by carbonate-rich, light-colored nannofossil ooze with clay, whereas glacials are characterized by clay- and diatom-rich, dark-colored clayey

nannofossil ooze or nannofossil clay. For most of the upper Miocene–Holocene section at Site 1208, the cycles are predominantly between nannofossil clay with diatoms and nannofossil ooze with clay and diatoms. The darker gray to green interbeds tend to have more abundant diatoms and clay, more dissolved calcareous plankton assemblages, and more abundant reduced iron minerals (i.e., pyrite). The lighter gray, tan, and white interbeds contain fewer diatoms, less clay, and a better-preserved calcareous plankton assemblage.

Upper Miocene–Holocene sediments recovered at Site 1208 contain few to common diatoms (up to 20%)—lower percentages than in sediments recovered at Site 1207 but higher percentages than contemporaneous units from sites on the Southern High of Shatsky Rise, where diatoms are usually <5%. Site 1208 is ~1° south of Site 1207 and ~4° north of the Southern High sites. As at Site 1207, diatom-rich layers are thought to represent intervals during which colder, more productive, transitional, and subarctic water masses shifted southward over the site. Lighter-colored layers that are poorer in diatoms represent warmer intervals during which Site 1208 was located in a subtropical water mass, similar to its location today and similar to sites on the Southern High through most of the Neogene. As the site is considerably higher than the surrounding deep-ocean floor, there may also be a topographic control on productivity.

Cyclic variations in the position of the lysocline and CCD have exerted a strong influence on the composition of sediment in the Pacific through the Cenozoic. At present, Site 1209, the shallowest on the Southern High, is situated well above the lysocline and CCD, which are at 3.5 and 4.1 km, respectively, in the region. As such, the uppermost Holocene sediments at Site 1209 have a relatively higher carbonate content than the Holocene of Sites 1207 (3.5 km) and 1208 (3.3 km). Because the CCD generally deepens in the Pacific during glacials (Farrell and Prell, 1989), its role in driving the Pleistocene lithologic cycles is probably minor. Instead, productivity and sediment transport may be more important. As with the deeper-water Sites 1207 and 1208, the darker-colored intervals generally contain higher amounts of biosiliceous material and clay and probably represent intervals of higher surface water productivity and increased in situ carbonate dissolution (e.g., Robinson and Jenkyns, this volume).

Even though the frequency of cycles in color reflectance through the Pleistocene are also related to glacial–interglacial cycles, the cycle amplitudes are smaller at Site 1209 than at deeper Site 1208 (Gylesjö, this volume), owing to a lower contribution of clay and siliceous microfossils to the sediment. Moreover, despite the shallower water depth, the sedimentation rate is significantly lower at Site 1209, ~13–14 m/m.y. over the Pleistocene compared to 42.4 m/m.y. at Site 1208. This indicates that carbonate production and preservation may have played a more important role in driving the Pleistocene lithologic cycles. As at the other sites, the dominant period of the cycles corresponds to eccentricity (100 k.y.) subsequent to 0.6 Ma and obliquity (41 k.y.) for the period from 0.6 to 2.5 Ma. The cycle wavelength at Site 1209, however, is much more irregular, suggesting that accumulation rates were highly variable through time.

Biostratigraphic age constraints suggest that the dominant cycle frequency over the last 0.6 m.y. is near that of the 100-k.y. eccentricity cycle. From 0.6 to 2.6 Ma, the dominant period shifts toward a higher frequency close to that associated with the 41-k.y. obliquity cycle. Throughout the last 2.6 m.y., the cycle amplitudes in reflectance re-

main remarkably similar between the Southern and Central Highs, although the mean total reflectance is higher on the Southern High. Climate-driven variations in opal and carbonate production and preservation and in clay fluxes are responsible for these changes. Analysis of the frequency of the dark–light cycles, calibrated to a well-established magnetostratigraphy throughout the rise, demonstrates that the dominant period of the cycles corresponding to obliquity (41 k.y.) extends back to 8 Ma (Evans et al., this volume). However, in the earlier Neogene section prior to the onset of Northern Hemisphere glaciation at 2.6 Ma, the amplitude of obliquity cycles is noticeably reduced, particularly at sites on the Southern High. The decrease results primarily from the absence of the low-carbonate "glacial" end-member of the cycles, despite a relative increase in silica content in the mid-Pliocene. The reduction in the high-frequency cycle amplitude is accompanied by an apparent increase in low-frequency cycle amplitude. In the Site 1209 color reflectance record (over the period 3–5 Ma), for example, there appears to be a long-wavelength oscillation with a period of roughly 1.0–1.25 m.y. Comparison with the derived orbital curves (Laskar, 1990) suggests that this cycle may be in phase with the long-period 1.25-m.y. obliquity cycle.

The peak in siliceous microfossil deposition at Site 1209 occurred in the mid-Pliocene, at roughly the same time as in regions of the North Pacific (Rea et al., 1995). The cyclic sedimentation during the Pleistocene and Pliocene is similar at Sites 1210 and 1211 and is characterized by relatively low amplitude cyclicity compared to the cyclic sedimentation recorded in the sediment farther north (e.g., Site 1209). This may be attributable to overall lower surface water productivity on the southern flank of the Southern High, as indicated by the diminished abundance of siliceous microfossils compared to sites farther north on the Southern, Central, and Northern Highs. In addition, the average sedimentation rate for the Pleistocene and Pliocene (8.6 m/m.y.) is significantly lower than those recorded at the Central and Northern Highs (up to 42 m/m.y.), also suggesting lower surface water productivity. However, despite the lower rates of primary productivity, the cyclicity was most likely dictated by small-scale changes in the intensity of surface water productivity. Relative biogenic silica enrichment occurs within the darker, more olive-green lithologies (up to 15% diatoms), with the lighter gray intervals remaining depleted in opal (~1%). It is unlikely that the light–dark sediment cycles resulted from glacial–interglacial fluctuations in deepwater corrosiveness given the relatively shallow water depth of ~2900 m, which lies above the subtropical northern Pacific CCD (Rea et al., 1995). In the Pleistocene Pacific Ocean, "glacial" intervals were generally times of higher productivity. Thus, the prominent color and compositional cycles are similar to those observed elsewhere in the North Pacific (Haug et al., 1995). Systematic changes in cycle amplitude and frequency are consistent from site to site, suggesting that these changes reflect regional paleoceanographic processes. The cycle packages (in all physical properties) are sufficiently distinct to allow for detailed correlation between sites.

Koizumi (1985) correlated fluctuations in Pliocene–Pleistocene diatom communities at DSDP sites in the abyssal plain northwest of Shatsky Rise to climatic fluctuations controlling the location of subarctic water masses at these sites. In colder intervals of the late Miocene to Pleistocene, the Northern High may have been within the transition zone between the subtropical water mass and the subarctic water mass, even though the site was well to the south of its current location. Thus,

fluctuations in the proportion of diatoms, which are more abundant in subarctic than subtropical waters, may reflect latitudinal shifts in the position of the transition zone.

If the darker layers correspond to cool intervals as argued, then the pattern of preservation is opposite that of most sites in the Pacific (e.g., Farrell and Prell, 1991; Zahn et al., 1991). A body of evidence suggests that during glacial stages intermediate deep waters were produced in the Pacific and that these young, nutrient-poor waters caused little dissolution close to their source. An opposite pattern was noted at a site on Emperor Seamount by Haug et al. (1995), who argued that the upwelling of nutrient- and $CO_2$-rich waters during glacial stages increased carbonate dissolution. Microfossils suggest a similar mechanism for dissolution patterns in the upper Miocene–Pleistocene at the Northern High site.

With the exception of Site 1214, all sites include complete and rapidly deposited Pliocene–Pleistocene sections in which the noncarbonate fraction forms a significant proportion, including the particularly expanded drift-deposit succession (200 m and 42.4 m/m.y. sedimentation rate) recovered at Site 1208. These sections, displaying visible cyclic sedimentary patterns, allowed better age assignments of magnetic chrons using astrochronology since 8 Ma (Evans et al., this volume, and study in progress).

# ACKNOWLEDGMENTS

# REFERENCES

Abbott, D.H., and Isley, A.E., 2002. Extraterrestrial influences on mantle plume activity. *Earth Planet. Sci. Lett.,* 205:53–62. doi:10.1016/S0012-821X(02)01013-0

Arthur, M.A., Dean, W.E., and Schlanger, S.O., 1985. Variations in the global carbon cycle during the Cretaceous related to climate, volcanism, and changes in atmospheric $CO_2$. *In* Sundquist, E.T., and Broecker, W.S. (Eds.), *The Carbon Cycle and Atmospheric CO$_2$: Natural Variations Archean to Present.* Geophys. Monogr., 32:504–529.

Arthur, M.A., Jenkyns, H.C., Brumsack, H.J., and Schlanger, S.O., 1988. Stratigraphy, geochemistry, and paleo-oceanography of organic carbon-rich Cretaceous sequences. *In* Ginsburg, R.N., and Beaudoin, B. (Eds.), *Cretaceous Resources, Events and Rhythms: Background and Plans for Research.* NATO ASI Ser., Ser. C, 304:75–119.

Aubry, M.-P., 1998. Early Palaeogene calcareous nannoplankton evolution: a tale of climatic amelioration. *In* Aubry, M.P., Lucas, S., and Berggren, W.A. (Eds.), *Late Paleocene–Early Eocene Climatic and Biotic Events in the Marine and Terrestrial Records:* New York (Columbia Univ. Press), 158–203.

Aubry, M.-P., and Ouda, K., 2003. Introduction. *In* Ouda, K., and Aubry, M.-P. (Eds.), *The Upper Paleocene–Lower Eocene of the Upper Nile Valley, Part 1. Stratigraphy:* New York (Micropaleontology Press), ii–iv.

Bains, S., Corfield, R.M., and Norris, R.D., 1999. Mechanisms of climate warming at the end of the Paleocene. *Science,* 285:724–727.

Barron, E.J., and Washington, W.M., 1985. Warm Cretaceous climates: high atmospheric $CO_2$ as a plausible mechanism. *In* Sundquist, E.T., and Broecker, W.S. (Eds.), *The Carbon Cycle and Atmospheric CO$_2$: Natural Variations Archean to Present.* Geophys. Monogr., 32:546–553.

Baudin, F., Deconinck, J.-F., Sachsenhofer, R.F., Strasser, A., and Arnaud, H., 1995. Organic geochemistry and clay mineralogy of Lower Cretaceous sediments from Allison and Resolution guyots (Sites 865 and 866), Mid-Pacific Mountains. *In* Winterer, E.L., Sager, W.W., Firth, J.V., and Sinton, J.M. (Eds.), *Proc. ODP, Sci. Results,* 143: College Station, TX (Ocean Drilling Program), 173–196.

Berggren, W.A., Kent, D.V., Swisher, C.C., III, and Aubry, M.-P., 1995. A revised Cenozoic geochronology and chronostratigraphy. *In* Berggren, W.A., Kent, D.V., Aubry, M.-P., and Hardenbol, J. (Eds.), *Geochronology, Time Scales and Global Stratigraphic Correlation.* Spec. Publ.—SEPM (Soc. Sediment. Geol.), 54:129–212.

Berner, R.A., 1994. GEOCARB II: a revised model of atms. $CO_2$ over Phanerozoic time. *Am. J. Sci.,* 294:56–91.

Bice, K.L., and Marotzke, J., 2001. Numerical evidence against reversed thermohaline circulation in the warm Paleocene/Eocene ocean. *J. Geophys. Res.,* 106(C6):11529–11542. doi:10.1029/2000JC000561

Bown, P.R., 2005. Selective calcareous nannoplankton survivorship at the Cretaceous–Tertiary Boundary. *Geology,* 33:653–656. doi:10.1130/G21566.1

Bralower, T.J., 2002. Evidence for surface water oligotrophy during the late Paleocene–Eocene Thermal Maximum: nannofossil assemblages data from Ocean Drilling Program Site 690, Maud Rise, Weddell Sea. *Paleoceanography,* 17(2):1–12. doi:10.1029/2001PA000662

Bralower, T.J., Ludwig, K.R., Obradovich, J.D., and Jones, D.L., 1990. Berriasian (Early Cretaceous) radiometric ages from the Grindstone Creek section, Sacramento Valley, California. *Earth Planet. Sci. Lett.,* 98:62–73.

Bralower, T.J., and Mutterlose, J., 1995. Calcareous nannofossil biostratigraphy of Site 865, Allison Guyot, Central Pacific Ocean: a tropical Paleogene reference section. *In* Winterer, E.L., Sager, W.W., Firth, J.V., and Sinton, J.M. (Eds.), *Proc. ODP, Sci. Results,* 143: College Station, TX (Ocean Drilling Program), 31–74.

Bralower, T.J., Premoli Silva, I., and Malone, M.J., 2002. New evidence for abrupt climate change in the Cretaceous and Paleogene: an Ocean Drilling Program expedition to Shatsky Rise, Northwest Pacific. *Geol. Soc. Am. Today,* 12(11):4–10.

Bralower, T.J., Premoli Silva, I., Malone, M.J., et al., 2002. *Proc. ODP, Init. Repts.,* 198 [Online]. Available from World Wide Web: <**http://www-odp.tamu.edu/publications/198_IR/198ir.htm**>

Bralower, T.J., Sliter, W.V., Arthur, M.A., Leckie, R.M., Allard, D.J., and Schlanger, S.O., 1993. Dysoxic/anoxic episodes in the Aptian–Albian (Early Cretaceous). *In* Pringle, M.S., Sager, W.W., Sliter, W.V., and Stein, S. (Eds.), *The Mesozoic Pacific: Geology, Tectonics, and Volcanism.* Geophys. Monogr., 77:5–37.

Bralower, T.J., Zachos, J.C., Thomas, E., Parrow, M., Paull, C.K., Kelly, D.C., Premoli Silva, I., Sliter, W.V., and Lohmann, K.C., 1995. Late Paleocene to Eocene paleoceanography of the equatorial Pacific Ocean: stable isotopes recorded at Ocean Drilling Program Site 865, Allison Guyot. *Paleoceanography,* 10(40):841–865.

Brass, G.W., Southam, J.R., and Peterson, W.H., 1982. Warm saline bottom water in the ancient ocean. *Nature (London, U. K.),* 296:620–623.

Brassell, S.C., Dumitrescu, M., and the ODP Leg 198 Shipboard Scientific Party, 2004. Recognition of alkenones in a lower Aptian porcellanite from the west-central Pacific. *Org. Geochem.,* 35:181–188.

Coffin, M.F., and Eldholm, O., 1994. Large igneous provinces: crustal structure, dimensions, and external consequences. *Rev. Geophys.,* 32:1–36.

Corfield, R.M., and Cartlidge, J.E., 1991. Isotopic evidence for the depth stratification of fossil and recent Globigerinina: a review. *Hist. Biol.,* 5:37–63.

Crouch, E.M., Heilmann-Clausen, C., Brinkhuis, H., Morgans, H.E.G., Rogers, K.M., Egger, H., and Schmitz, B., 2001. Global dinoflagellate event associated with the Late Paleocene Thermal Maximum. *Geology,* 29:315–318.

Dickens, G.R., 2000. Methane oxidation during the late Palaeocene Thermal Maximum. *Bull. Soc. Geol. Fr.,* 171:37–49.

Dickens, G.R., Castillo, M.M., and Walker, J.G.C., 1997. A blast of gas in the latest Paleocene: simulating first-order effects of massive dissociation of oceanic methane hydrate. *Geology,* 25(3):259–262. **doi:10.1130/0091-7613(1997)025<0259:ABOGIT>2.3.CO;2**

Dickens, G.R., O'Neil, J.R., Rea, D.K., and Owen, R.M., 1995. Dissociation of oceanic methane hydrate as a cause of the carbon isotope excursion at the end of the Paleocene. *Paleoceanography,* 10:965–972. **doi:10.1029/95PA02087**

Dumitrescu, M., and Brassell, S.C., 2005. Biogeochemical assessment of sources of organic matter and paleoproductivity during the early Aptian oceanic anoxic event at Shatsky Rise, ODP Leg 198. *Org. Geochem.,* 36:1002–1022. **doi:10.1016/j.orggeochem.2005.03.001**

Dutton, A., Lohmann, K.C., and Leckie, R.M., 2005. Insights from the Paleogene tropical Pacific: foraminiferal stable isotope and elemental results from Site 1209, Shatsky Rise. *Paleoceanography,* 20. **doi:10.1029/2004PA001098**

Erbacher, J., and Thurow, J., 1997. Influence of oceanic anoxic events on the evolution of mid-Cretaceous radiolaria in the North Atlantic and western Tethys. *Mar. Micropalaeontol.,* 30:139–158. **doi:10.1016/S0377-8398(96)00023-0**

Erez, J., and Luz, B., 1983. Experimental paleotemperature equation for planktonic foraminifera. *Geochim. Cosmochim. Acta,* 47:1025–1031. **doi:10.1016/0016-7037(83)90232-6**

Farrell, J.W., and Prell, W.L., 1989. Climatic change and $CaCO_3$ preservation: an 800,000 year bathymetric reconstruction from the central equatorial Pacific Ocean. *Paleoceanography,* 4(4):447–466.

Farrell, J.W., and Prell, W.L., 1991. Pacific $CaCO_3$ preservation and $\delta^{18}O$ since 4 Ma: paleoceanic and paleoclimatic implications. *Paleoceanography,* 6:485–498.

Fischer, A.G., Heezen, B.C., et al., 1971. *Init. Repts. DSDP,* 6: Washington (U.S. Govt. Printing Office).

Fitton, J.G., and Godard, M., 2004. Origin and evolution of magmas on the Ontong Java Plateau. *In* Fitton, J.G., Mahoney, J.J., Wallace, P.J., and Saunders, A.D. (Eds.), *Origin and Evolution of the Ontong Java Plateau.* Geol. Soc. Spec. Publ., 229:151–178.

Frank, T.D., Thomas, D.J., Leckie, R.M., Arthur, M.A., Bown, P.R., Jones, K., and Lees, J.A., 2005. The Maastrichtian record from Shatsky Rise (northwest Pacific): a tropical perspective on global ecological and oceanographic changes. *Paleoceanography,* 20. **doi:10.1029/2004PA001052**

Gibbs, S.J., Bralower, T.J., Bown, P.R., Zachos, J.C., and Bybell, L., 2006. Shelf-open ocean calcareous phytoplankton assemblages across the Paleocene-Eocene Thermal Maximum: implications for global productivity gradients. *Geology,* 34:233–236.

Gibson, T.G., Bybell, L.M., and Owens, J.P., 1993. Latest Paleocene lithologic and biotic events in neritic deposits of southwestern New Jersey. *Paleoceanography,* 8:495–514.

Gradstein, F.M., Ogg, J.G., and Smith, A. (Eds.), 2004. *A Geologic Time Scale 2004:* Cambridge (Cambridge Univ. Press).

Haug, G.H., Maslin, M.A., Sarnthein, M., Stax, R., and Tiedemann, R., 1995. Evolution of northwest Pacific sedimentation patterns since 6 Ma (Site 882). *In* Rea, D.K., Basov, I.A., Scholl, D.W., and Allan, J.F. (Eds.), *Proc. ODP, Sci. Results,* 145: College Station, TX (Ocean Drilling Program), 293–314.

Heath, G.R., Burckle, L.H., et al., 1985. *Init. Repts. DSDP,* 86: Washington (U.S. Govt. Printing Office).

Hooker, J.J., 1996. Mammalian biostratigraphy across the Paleocene–Eocene boundary in the Paris, London and Belgian basins. *In* Knox, R.O., Corfield, R.M., and Dunay, R.E. (Eds.), *Correlation of the Early Paleogene in Northwest Europe.* Geol. Soc. Spec. Publ., 101:205–218.

Huber, M., and Sloan, L.C., 1999. Warm climate transitions: a general circulation modeling study of the Late Paleocene Thermal Maximum (~56 Ma). *J. Geophys. Res.,* 104:16633–16656. **doi:10.1029/1999JD900272**

Ingle, S., and Coffin, M., 2004. Impact origin of the greater Ontong Java Plateau? *Earth Planet. Sci. Lett.,* 218:123–134. **doi:10.1016/S0012-821X(03)00629-0**

Jenkyns, H.C., 1980. Cretaceous anoxic events: from continents to oceans. *J. Geol. Soc. (London, U. K.),* 137:171–188.

Jenkyns, H.C., 1995. Carbon-isotope stratigraphy and paleoceanographic significance of the Lower Cretaceous shallow-water carbonates of Resolution Guyot, Mid-Pacific Mountains. *In* Winterer, E.L., Sager, W.W., Firth, J.V., and Sinton, J.M. (Eds.), *Proc. ODP, Sci. Results,* 143: College Station, TX (Ocean Drilling Program), 99–104.

Katz, M.E., Pak, D.K., Dickens, G.R., and Miller, K.G., 1999. The source and fate of massive carbon input during the Latest Paleocene Thermal Maximum. *Science,* 286:1531–1533. **doi:10.1126/science.286.5444.1531**

Keller, G., 1988. Extinction, survivorship and evolution of planktic foraminifers across the Cretaceous/Tertiary boundary at El Kef, Tunisia. *Mar. Micropaleontol.,* 13:239–263. **doi:10.1016/0377-8398(88)90005-9**

Kelly, D.C., Bralower, T.J., and Zachos, J.C., 1998. Evolutionary consequences of the Latest Paleocene Thermal Maximum for tropical planktonic foraminifera. *Palaeogeogr., Palaeoclimatol., Palaeoecol.,* 141:139–161. **doi:10.1016/S0031-0182(98) 00017-0**

Kelly, D.C., Bralower, T.J., Zachos, J.C., Premoli Silva, I., and Thomas, E., 1996. Rapid diversification of planktonic foraminifera in the tropical Pacific (ODP Site 865) during the Late Paleocene Thermal Maximum. *Geology,* 24:423–426.

Kennett, J.P., Keller, G., and Srinivasan, M.S., 1985. Miocene planktonic foraminiferal biogeography and paleoceanographic development of the Indo-Pacific region. *In* Kennett, J.P. (Ed.), *The Miocene Ocean: Paleoceanography and Biogeography.* Mem.— Geol. Soc. Am., 163:197–236.

Kennett, J.P., and Stott, L.D., 1991. Abrupt deep-sea warming, paleoceanographic changes and benthic extinctions at the end of the Palaeocene. *Nature (London, U. K.),* 353:225–229. **doi:10.1038/353225a0**

Kent, D.V., Cramer, B.S., Lanci, L., Wang, D., Wright, J.D., and Van der Voo, R., 2003. A case for a comet impact trigger for the Paleocene/Eocene Thermal Maximum and carbon isotope excursion. *Earth Planet. Sci. Lett.,* 211:13–26. **doi:10.1016/S0012-821X(03)00188-2**

Koeberl, C., Armstrong, R.A., and Reimold, W.U., 1997. Morokweng, South Africa: a large impact structure of Jurassic–Cretaceous boundary age. *Geology,* 25:731–734. **doi:10.1130/0091-7613(1997)025<0731:MSAALI>2.3.CO;2**

Koizumi, I., 1985. Late Neogene paleoceanography in the western north Pacific. *In* Heath, G.R., Burckle, L.H., et al., *Init. Repts. DSDP,* 86: Washington (U.S. Govt. Printing Office), 86:429–438.

Larson, R.L., 1991. Geological consequences of superplumes. *Geology,* 19:963–966.

Larson, R.L., and Erba, E., 1999. Onset of the Mid-Cretaceous greenhouse in the Barremian–Aptian: igneous events and the biological, sedimentary and geochemical responses. *Paleoceanography,* 14:663–678. **doi:10.1029/1999PA900040**

Larson, R.L., Moberly, R., et al., 1975. *Init. Repts. DSDP,* 32: Washington (U.S. Govt. Printing Office).

Laskar, J., 1990. The chaotic motion of the solar system: a numerical estimate of the size of the chaotic zones. *Icarus,* 88:266–291. **doi:10.1016/0019-1035(90)90084-M**

Leckie, R.M., Bralower, T.J., and Cashman, R., 2002. Oceanic anoxic events and plankton evolution: biotic response to tectonic forcing during the mid-Cretaceous. *Paleoceanography,* 17(3). **doi:10.1029/2001PA000623**

Lourens, L.J., Sluijs, A., Kroon, D., Zachos, J.C., Thomas, E., Röhl, U., Bowles, J., and Raffi, I., 2005. Astronomical pacing of late Palaeocene to early Eocene global warming events. *Nature (London, U. K.),* 435:1083–1087. **doi:10.1038/nature03814**

MacLeod, K.G., and Huber, B.T., 1996. Reorganization of deep ocean circulation accompanying a Late Cretaceous extinction event. *Nature (London, U. K.),* 380:422–425. **doi:10.1038/380422a0**

MacLeod, K.G., Huber, B.T., and Ward, P.D., 1996. The biostratigraphy and paleobiogeography of Maastrichtian inoceramids. *In* Ryder, G., Fastowsky, D., and Gartner, S. (Eds.), *The Cretaceous–Tertiary Event and Other Catastrophes in Earth History.* Spec. Publ.–Geol. Soc. Am., 307:361–373.

Mahoney, J.J., Duncan, R.A., Tejada, M.L.G., Sager, W.W., and Bralower, T.J., 2005. Jurassic–Cretaceous boundary age and mid-ocean-ridge-type mantle source for Shatsky Rise. *Geology,* 33:185–188. **doi:10.1130/G21378.1**

Mahoney, J.J., and Spencer, K.J., 1991. Isotopic evidence for the origin of the Manihiki and Ontong Java oceanic plateaus. *Earth Planet. Sci. Lett.,* 104:196–210.

Maslin, M.A., Haug, G.H., Sarnthein, M., Tiedemann, R., Erlenkeuser, H., and Stax, R., 1995. Northwest Pacific Site 882: the initiation of Northern Hemisphere glaciation. *In* Rea, D.K., Basov, I.A., Scholl, D.W., and Allan, J.F. (Eds.), *Proc. ODP, Sci. Results,* 145: College Station, TX (Ocean Drilling Program), 315–329.

Menegatti, A.P., Weissert, H., Brown, R.S., Tyson, R.V., Farrimond, P., Strasser, A., and Caron, M., 1998. High resolution $\delta^{13}$C stratigraphy through the early Aptian "Livello Selli" of the Alpine Tethys. *Paleoceanography,* 13:530–545. **doi:10.1029/98PA01793**

Nakanishi, M., Sager, W.W., and Klaus, A., 1999. Magnetic lineations within Shatsky Rise, northwest Pacific Ocean: implications for hot spot–triple junction interaction and oceanic plateau formation. *J. Geophys. Res.,* 104:7539–7556. **doi:10.1029/1999JB900002**

Natland, J.H., 1993. Volcanic ash and pumice at Shatsky Rise: sources, mechanisms of transport, and bearing on atmospheric circulation. *In* Natland, J.H., Storms, M.A., et al., *Proc. ODP, Sci. Results,* 132: College Station, TX (Ocean Drilling Program), 57–66.

Natland, J.H., Storms, M.A., et al., 1993. *Proc. ODP, Sci. Results,* 132: College Station, TX (Ocean Drilling Program).

Norris, R.D., and Röhl, U., 1999. Carbon cycling and chronology of climate warming during the Palaeocene/Eocene transition. *Nature (London, U. K.),* 401:775–778. **doi:10.1038/44545**

Olsson, R.K., Hemleben, C., Berggren, W.A., and Huber, B.T. (Eds.), 1999. *Atlas of Paleocene Planktonic Foraminifera.* Smithson. Contrib. Paleobiol., Vol. 85.

Pak, D.K., and Miller, K.G., 1992. Paleocene to Eocene benthic foraminiferal isotopes and assemblages: implications for deepwater circulation. *Paleoceanography,* 7:405–422.

Pálfy, J., Smith, P.L., and Mortensen, J.K., 2000. A U-Pb and $^{40}$Ar-$^{39}$Ar time scale for the Jurassic. *Can. J. Earth Sci.,* 37:923–944. **doi:10.1139/cjes-37-6-923**

Pospichal, J.J., 1996. Calcareous nannoplankton mass extinction at the Cretaceous/Tertiary boundary: an update. *In* Ryder, G., et al. (Eds.), *The Cretaceous–Tertiary Event and Other Catastrophes in Earth History.* Spec. Pap.—Geol. Soc. Am., 307:335–360.

Ravizza, G., Norris, R.N., Blusztajn, J., and Aubry, M.-P., 2001. An osmium isotope excursion associated with the Late Paleocene Thermal Maximum: evidence of intensified chemical weathering. *Paleoceanography,* 16:155–163. **doi:10.1029/2000PA000541**

Ray, J.S., Mahoney, J.J., Johnson, K.T.M., Pyle, D.G., Naar, D., and Wessel, P., 2003. Geochemistry of volcanism along the Nazca Ridge and Easter Seamount Chain [EGS-AGU-EUG Joint Assembly, Nice, 06–11 April 2003].

Rea, D.K., Basov, I.A., Krissek, L.A., and the Leg 145 Scientific Party, 1995. Scientific results of drilling the North Pacific Transect. *In* Rea, D.K., Basov, I.A., Scholl, D.W., and Allan, J.F. (Eds.), *Proc. ODP, Sci. Results,* 145: College Station, TX (Ocean Drilling Program), 577–596.

Rea, D.K., and Leinen, M., 1985. Neogene history of the calcite compensation depth and lysocline in the South Pacific Ocean. *Nature (London, U. K.),* 316:805–807. **doi:10.1038/316805a0**

Robinson, S.A., Williams, T., and Bown, P.R., 2004. Fluctuations in biosiliceous production and the generation of Early Cretaceous oceanic anoxic events in the Pacific Ocean (Shatsky Rise, ODP Leg 198). *Paleoceanography,* 19(PA4024). **doi:10.1029/2004PA001010**

Rogers, G.C., 1982. Oceanic plateaus as meteorite impact signatures. *Nature (London, U. K.),* 299:341–342. **doi:10.1038/299341a0**

Romine, K., and Lombari, G., 1985. Evolution of Pacific circulation in the Miocene: radiolarian evidence from DSDP Site 289. *In* Kennett, J.P. (Ed.), *The Miocene Ocean: Paleoceanography and Biogeography.* Mem.—Geol. Soc. Am., 163:273–290.

Sager, W.W., in press. What built Shatsky Rise, a mantle plume or ridge processes? *In* Foulger, G.R., Anderson, D.L., Natland, J.H., and Presnall, D.C. (Eds.), *Plumes, Plates, and Paradigms.* Spec. Pap.—Geol. Soc. Am.

Sager, W.W., and Han, H.-C., 1993. Rapid formation of the Shatsky Rise oceanic plateau inferred from its magnetic anomaly. *Nature (London, U. K.),* 364:610–613. **doi:10.1038/364610a0**

Sager, W.W., Kim, J., Klaus, A., Nakanishi, M., and Khankishieva, L.M., 1999. Bathymetry of Shatsky Rise, northwest Pacific Ocean: implications for ocean plateau development at a triple junction. *J. Geophys. Res., [Solid Earth Planets],* 104(4):7557–7576.

Scher, H.D., and Martin, E.E., 2004. Circulation in the Southern Ocean during the Paleogene inferred from neodymium isotopes. *Earth Planet. Sci. Lett.,* 228:391–405. **doi:10.1016/j.epsl.2004.10.016**

Schlanger, S.O., Arthur, M.A., Jenkyns, H.C., and Scholle, P.A., 1987. The Cenomanian–Turonian oceanic anoxic event, I. Stratigraphy and distribution of organic carbon-rich beds and the marine $\delta^{13}$C excursion. *In* Brooks, J., and Fleet, A.J. (Eds.), *Marine Petroleum Source Rocks.* Spec. Publ.—Geol. Soc. London, 26:371–399.

Schlanger, S.O., and Douglas, R.G., 1974. The pelagic ooze-chalk-limestone transition and its implication for marine stratigraphy. *In* Hsü, K.J., and Jenkyns, H.C. (Eds.), *Pelagic Sediments: On Land and Under the Sea.* Spec. Publ.—Int. Assoc. Sedimentol., 1:117–148.

Schlanger, S.O., and Jenkyns, H.C., 1976. Cretaceous oceanic anoxic events: causes and consequences. *Geol. Mijnbouw,* 55:179–184.

Sinton, C.W., and Duncan, R.A., 1997. Potential links between ocean plateau volcanism and global ocean anoxia at the Cen/Tur boundary. *Econ. Geol.,* 92:836–842.

Sliter, W.V., 1989. Aptian anoxia in the Pacific Basin. *Geology,* 17:909–912. **doi:10.1130/0091-7613(1989)017<0909:AAITPB>2.3.CO;2**

Snow, L.J., Duncan, R.A., and Bralower, T.J., 2005. Trace element abundances in the Rock Canyon anticline, Pueblo, Colorado marine sedimentary section and their relationship to Caribbean Plateau construction and oxygen anoxic event 2. *Paleoceanography,* 20. **doi:10.1029/2004PA001093**

Speijer, R.P., and Schmitz, B., 1998. A benthic foraminiferal record of Paleocene sea-level changes and trophic conditions at Gebel Aweina, Egypt. *Palaeogeogr., Palaeoclimatol., Palaeoecol.,* 137:79–101. **doi:10.1016/S0031-0182(97)00107-7**

Sun, S.-S., and McDonough, W.F., 1989. Chemical and isotopic systematics of oceanic basalts: implications for mantle composition and processes. *In* Saunders, A.D., and Norry, M.J. (Eds.), *Magmatism in the Ocean Basins.* Geol. Soc. Spec. Publ., 42:313–345.

Svenson, H., Planke, S., Malthe-Sørenssen, A., Jamtveit, B., Myklebust, R., Eidem, T.R., and Rey, S.S., 2004. Release of methane from a volcanic basin as a mechanism for initial Eocene global warming. *Nature (London, U. K.),* 429:542–545. **doi:10.1038/nature02566**

Taylor, B., Fujioka, K., et al., 1990. *Proc. ODP, Init. Repts.,* 126: College Station, TX (Ocean Drilling Program).

Tejada, M.L.G., Mahoney, J.J., Castillo, P.R., Ingle, S.P., Sheth, H.C., and Weis, D., 2004. Pin-pricking the elephant: evidence on the origin of the Ontong Java Plateau from Pb-Sr-Hf-Nd isotopic characteristics of ODP Leg 192 basalts. *In* Fitton, J.G., Mahoney, J.J., Wallace, P.J., and Saunders, A.D. (Eds.), *Origin and Evolution of the Ontong Java Plateau.* Geol. Soc. Spec. Publ., 229:133–150.

Thierstein, H.R., and Okada, H., 1979. The Cretaceous/Tertiary boundary event in the North Atlantic. *In* Tucholke, B.E., Vogt, P.R., et al., *Init. Repts. DSDP,* 43: Washington (U.S. Govt. Printing Office), 601–616.

Thomas, D.J., 2004. Evidence for deep-water production in the North Pacific Oceans during the early Cenozoic warm interval. *Nature (London, U. K.),* 430:65–68. **doi:10.1038/nature02639**

Thomas, D.J., 2005. Reconstruction of ancient deep-sea circulation patterns using the Nd isotopic composition of fossil fish debris. *Geol. Soc. Spec. Publ.,* 395:1–12.

Thomas, E., 1990. Late Cretaceous–early Eocene mass extinctions in the deep sea. *In* Sharpton, V.L., and Ward, P.D. (Eds.), *Global Catastrophes in Earth History: An Interdisciplinary Conference on Impacts, Volcanism, and Mass Mortality.* Spec. Pap.—Geol. Soc. Am., 247:481–495.

Thomas, E., 1998. Biogeography of the late Paleocene benthic foraminiferal extinction. *In* Aubry, M.-P., Lucas, S.G., and Berggren, W.A., (Eds.), *Late Paleocene–Early Eocene Biotic and Climatic Events in the Marine and Terrestrial Records:* New York (Columbia Univ. Press), 214–243.

Thomas, E., 2003. Extinction and food on the seafloor: a high-resolution benthic foraminiferal record across the initial Eocene thermal maximum, Southern Ocean Site 690. *In* Wing, S.L., Gingerich, P.D., Schmitz, B., and Thomas, E. (Eds.), *Causes and Consequences of Globally Warm Climates in the Early Paleogene,* Spec. Pap.—Geol. Soc. Am., 369:319–332.

Thomas, E., and Shackleton, N.J., 1996. The latest Paleocene benthic foraminiferal extinction and stable isotope anomalies. *In* Knox, R.O., Corfield, R.M., and Dunay,

R.E., (Eds.), *Correlation of the early Paleogene in Northwest Europe.* Geol. Soc. Spec. Publ. London, 101:401–441.

Thomas, E., Zachos, J.C., and Bralower, T.J., 2000. Ice-free to glacial world transition as recorded by benthic foraminifera. *In* Huber, B.T., MacLeod, K.G., and Wing, S.L. (Eds.), *Warm Climates in Earth History:* Cambridge (Cambridge Univ. Press), 132–160.

Tjalsma, R.C., and Lohmann, G.P., 1983. *Paleocene–Eocene Bathyal and Abyssal Benthic Foraminifera from the Atlantic Ocean.* Micropaleontology, Spec. Publ., 4:1–90.

Tripati, A.K., Delaney, M.L., Zachos, J.C., Anderson, L.D., Kelly, D.C., and Elderfield, H., 2003. Tropical sea-surface temperature reconstruction for the early Paleogene using Mg/Ca ratios of planktonic foraminifera. *Paleoceanography,* 18. doi:10.1029/2003PA000937

Vogt, P.R., 1989. Volcanogenic upwelling of anoxic, nutrient-rich water: a possible factor in carbonate-bank/reef demise and benthic faunal extinctions? *Geol. Soc. Am. Bull.,* 101:1225–1245.

Walker, J.C.G., and Kasting, J.F., 1992. Effects of fuel and forest conservation on future levels of atmospheric carbon dioxide. *Global Planet. Change,* 5:151–189.

Wilson, P.A., and Norris, R.D., 2001. Warm tropical ocean surface and global anoxia during the mid-Cretaceous period. *Nature (London, U. K.),* 412:425–429. doi:10.1038/35086553

Zachos, J.C., Kroon, D., Blum, P., et al., 2004. *Proc. ODP, Init. Repts.,* 208 [CD-ROM]. Available from: Ocean Drilling Program, Texas A&M University, College Station TX 77845-9547, USA. [HTML]

Zachos, J.C., Lohmann, K.C., Walker, J.C.G., and Wise, S.W., Jr., 1993. Abrupt climate changes and transient climates during the Paleogene: a marine perspective. *J. Geol.,* 101:191–213.

Zachos, J.C., Pagani, M., Sloan, L., Thomas, E., and Billups, K., 2001. Trends, rhythms, and aberrations in global climate 65 Ma to present. *Science,* 292:686–693. doi:10.1126/science.1059412

Zachos, J.C., Röhl, U., Schellenberg, S.A., Sluijs, A., Hodell, D.A., Kelly, D.C., Thomas, E., Nicolo, M., Raffi, I., Lourens, L.J., McCarren, H., and Kroon, D., 2005. Rapid acidification of the ocean during the Paleocene–Eocene Thermal Maximum. *Science,* 308:1611–1615. doi:10.1126/science.1109004

Zachos, J.C., Wara, M.W., Bohaty, S., Delaney, M.L., Petrizzo, M.R., Brill, A., Bralower, T.J., and Premoli-Silva, I., 2003. A transient rise in tropical sea surface temperature during the Paleocene–Eocene Thermal Maximum. *Science,* 302:1551–1554. doi:10.1126/science.1090110

Zahn, R., Rushdi, A., Pisias, N.G., Bornhold, B.D., Blaise, B., and Karlin, R., 1991. Carbonate deposition and benthic $\delta^{13}C$ in the subarctic Pacific: implications for changes of the oceanic carbonate system during the past 750,000 years. *Earth Planet. Sci. Lett.,* 103:116–132.

**Figure F1.** Bathymetric map of Shatsky Rise showing location of Leg 198 sites. Site 1207 is located on the Northern High, Site 1208 is on the Central High, and Sites 1209–1214 are on the Southern High (modified from Bralower, Premoli Silva, Malone, et al., 2002).
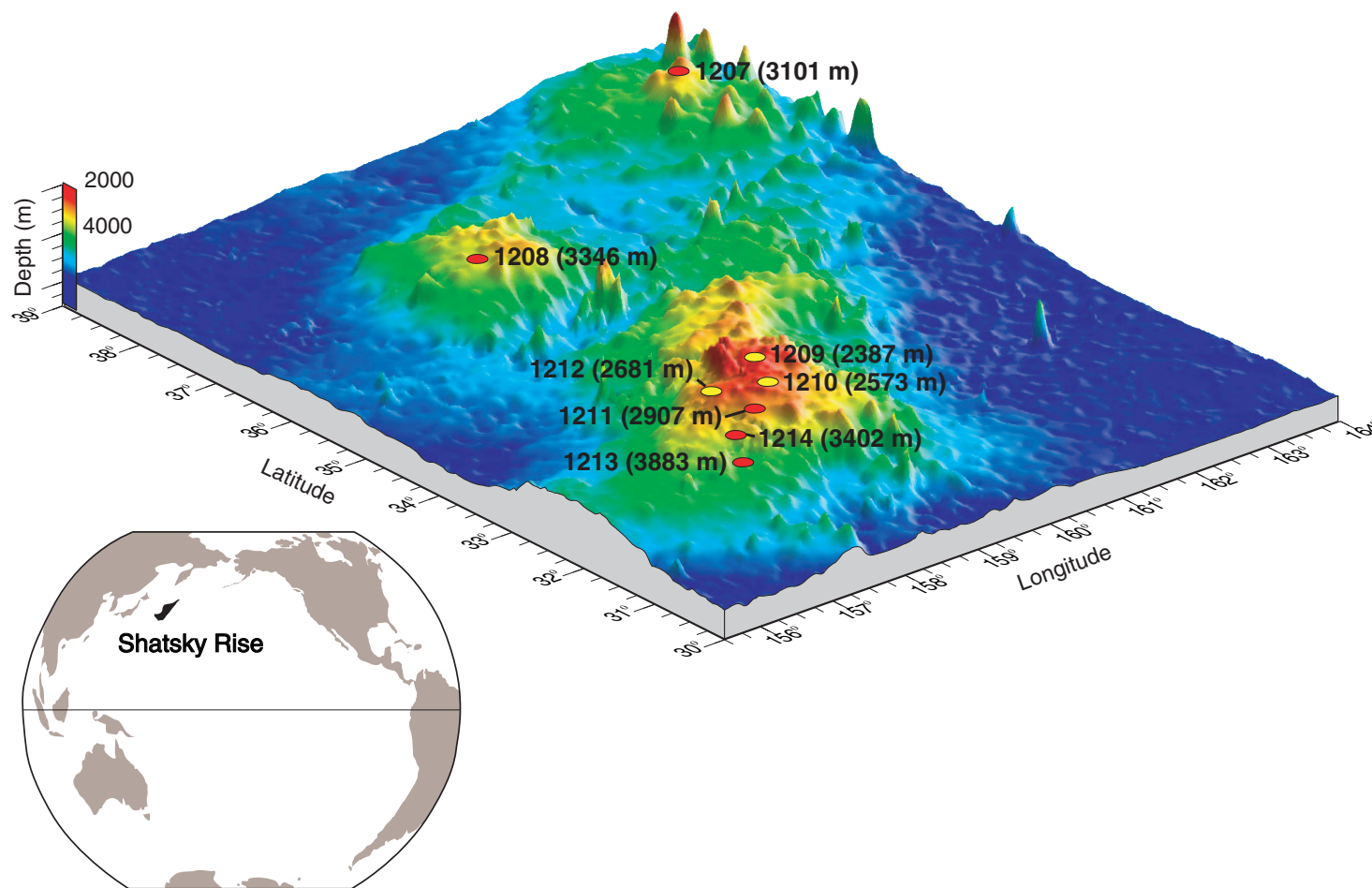
**Figure F2.** Generalized climate curve for the Cretaceous and Paleogene derived from deep-sea benthic oxygen isotope data (from Zachos et al., 1993, 2001). Also shown are locations of events discussed including Eocene/Oligocene transition, Paleocene/Eocene Thermal Maximum (PETM), late Paleocene biotic event, Cretaceous/Tertiary boundary (K/T), mid-Maastrichtian event (MME), and early Aptian Oceanic Anoxic Event (OAE1a) (modified from Bralower, Premoli Silva, Malone, et al., 2002).
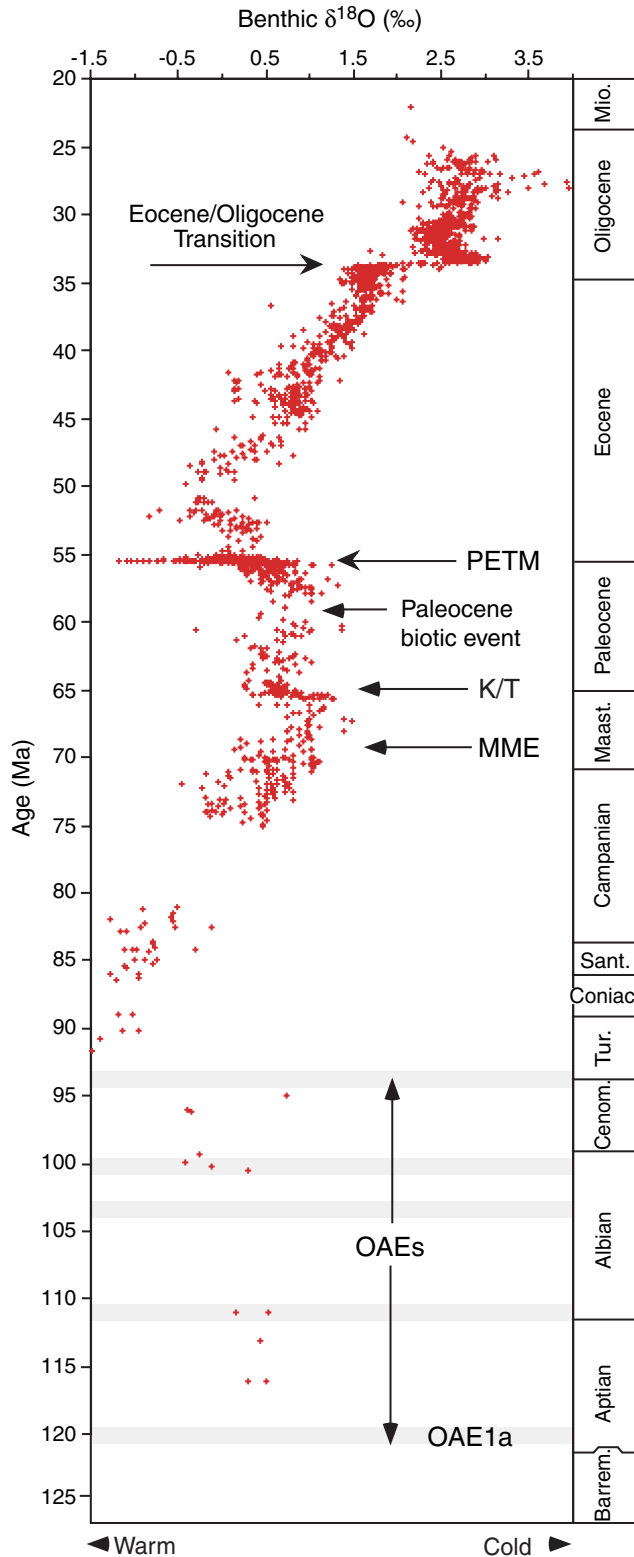
**Figure F3.** Summary of stratigraphy and lithologic succession from Sites 1207–1214. Lithology is plotted against time to show duration of periods of deposition and location of unconformities. Southern High Sites 1209–1214 are ordered by water depth. Arrows show stratigraphic position of transient events discussed: Eocene/Oligocene (E/O) transition, Paleocene/Eocene Thermal Maximum (PETM), late Paleocene biotic event, Cretaceous/Tertiary boundary (K/T), mid-Maastrichtian event (MME), and early Aptian Oceanic Anoxic Event (OAE1a) (modified from Bralower, Premoli Silva, Malone, et al., 2002).
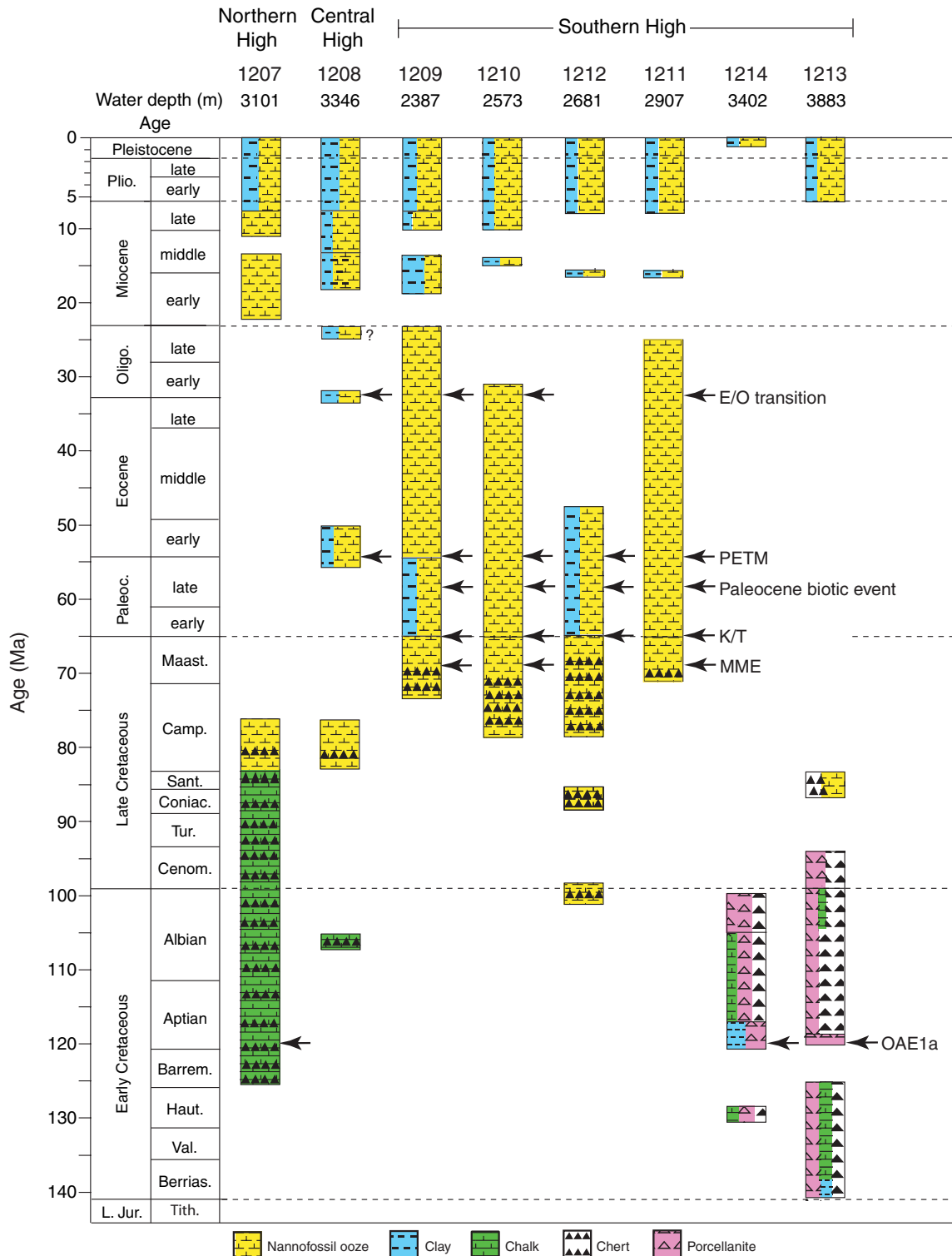
**Figure F4.** Stratigraphic synthesis for Shatsky Rise sites from 145 to 130 Ma plotted against the biostratigraphic scheme used in Bralower, Premoli Silva, Malone, et al. (2002). Biostratigraphy after Bralower, Premoli Silva, Malone, et al. (2002) and **Bown** (this volume). Condensed pattern annotates intervals in which some biozones could not be identified with certainty and/or may comprise short hiatuses or unconformities. Note that in the Cretaceous sections older than Campanian the recovery was very poor due to diffuse chert layers alternating with softer chalk. OAE = Ocean Anoxic Event, TD = total depth.
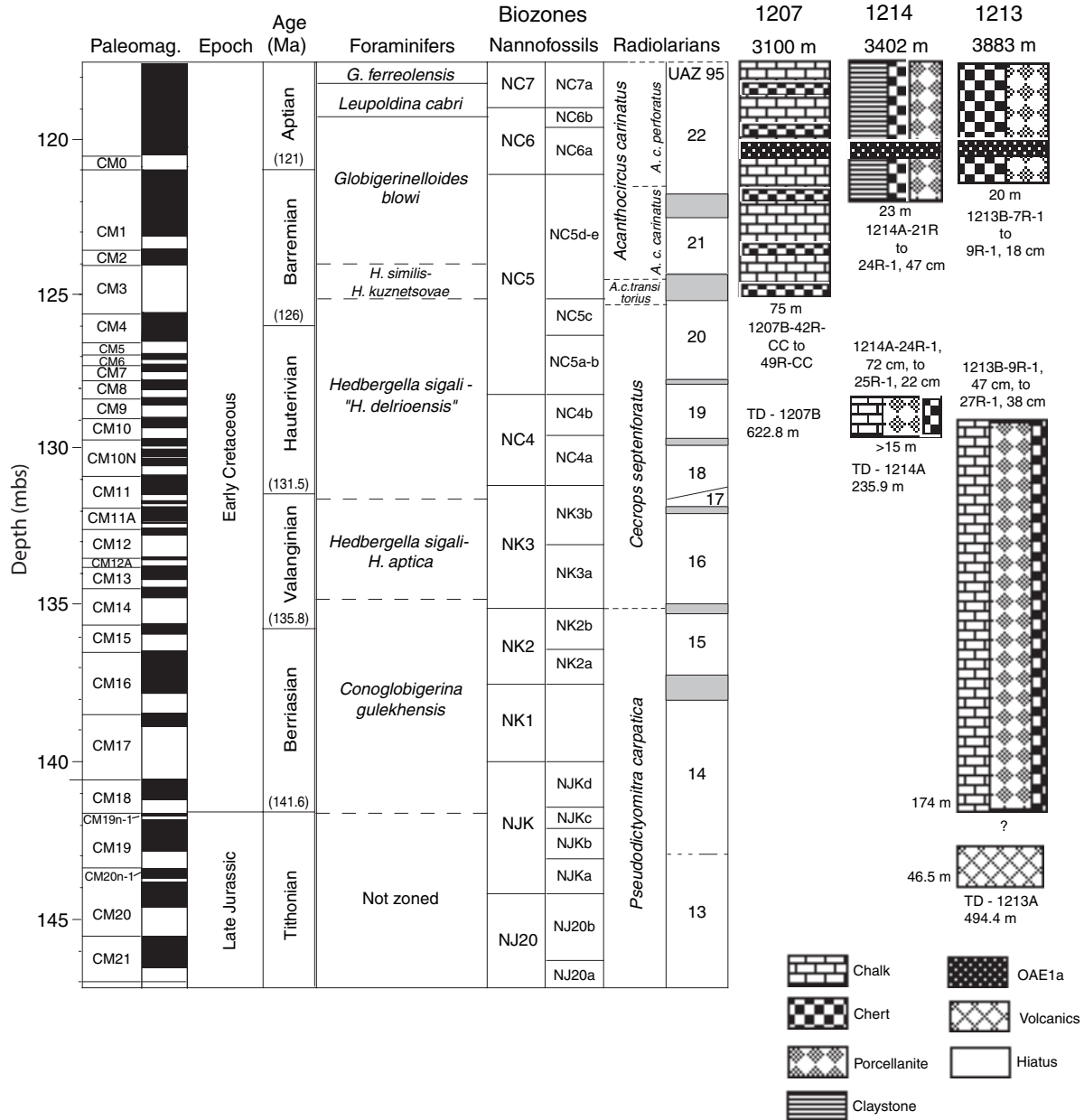
**Figure F5.** Stratigraphic summary for 130–80 Ma. Biostratigraphy after Bralower, Premoli Silva, Malone, et al. (2002), **Bown** (this volume), and **Lees and Bown** (this volume). Condensed pattern annotates intervals in which some biozones could not be identified with certainty and/or may comprise short hiatuses or unconformities. Note that in the Cretaceous sections older than Campanian the recovery was very poor due to diffuse chert layers alternating with softer chalk. OAE = Ocean Anoxic Event, TD = total depth.
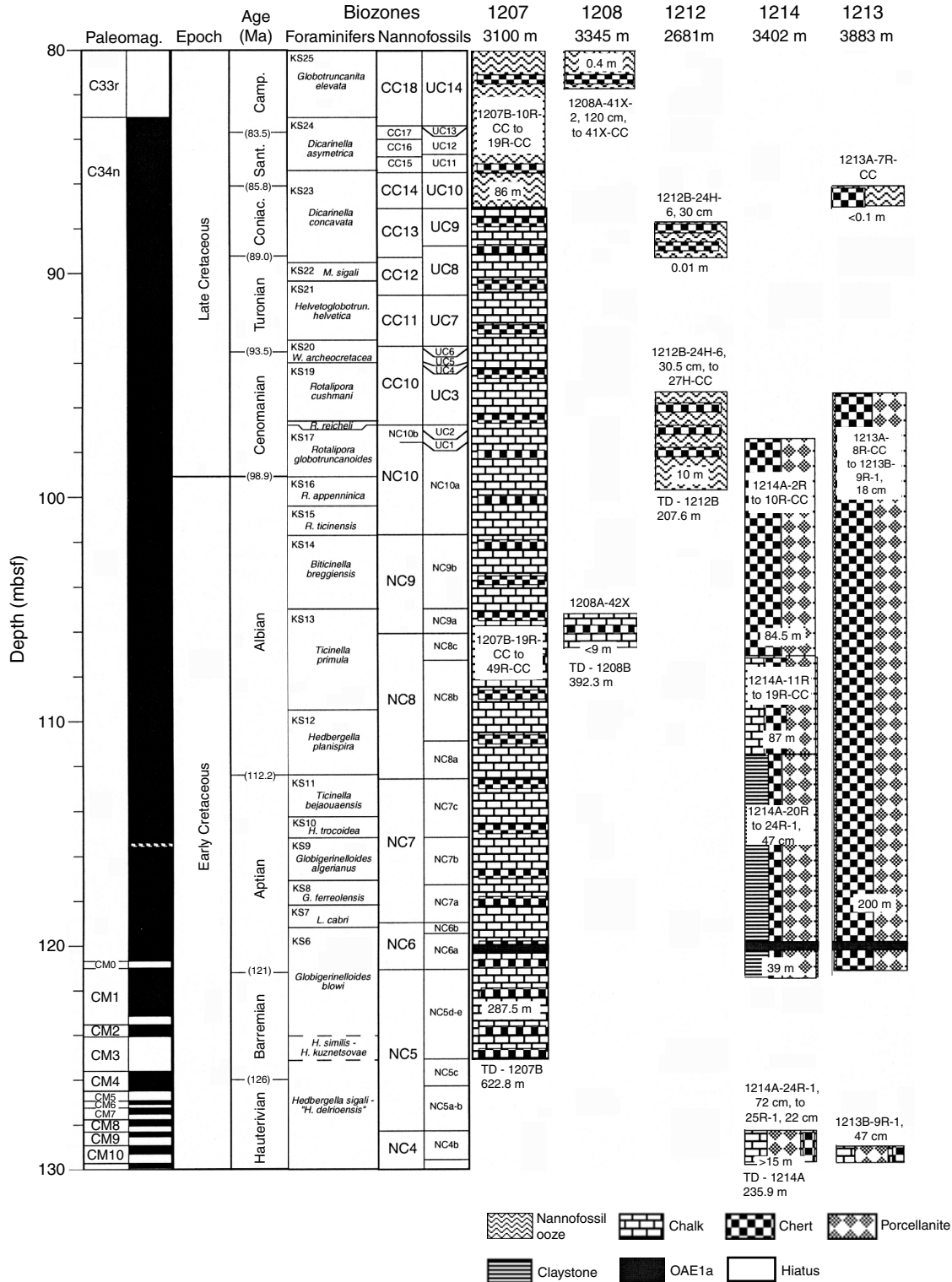
**Figure F6.** Stratigraphic summary for 85–60 Ma. Biostratigraphy after Bralower, Premoli Silva, Malone, et al. (2002), **Lees and Bown** (this volume), **Bralower** (this volume), **Petrizzo et al.** (this volume), and **Premoli Silva et al.** (this volume). Condensed pattern annotates intervals in which some biozones could not be identified with certainty and/or may comprise short hiatuses or unconformities. Note that in the Cretaceous sections older than Campanian the recovery was very poor due to diffuse chert layers alternating with softer chalk. OAE = Ocean Anoxic Event, TD = total depth.
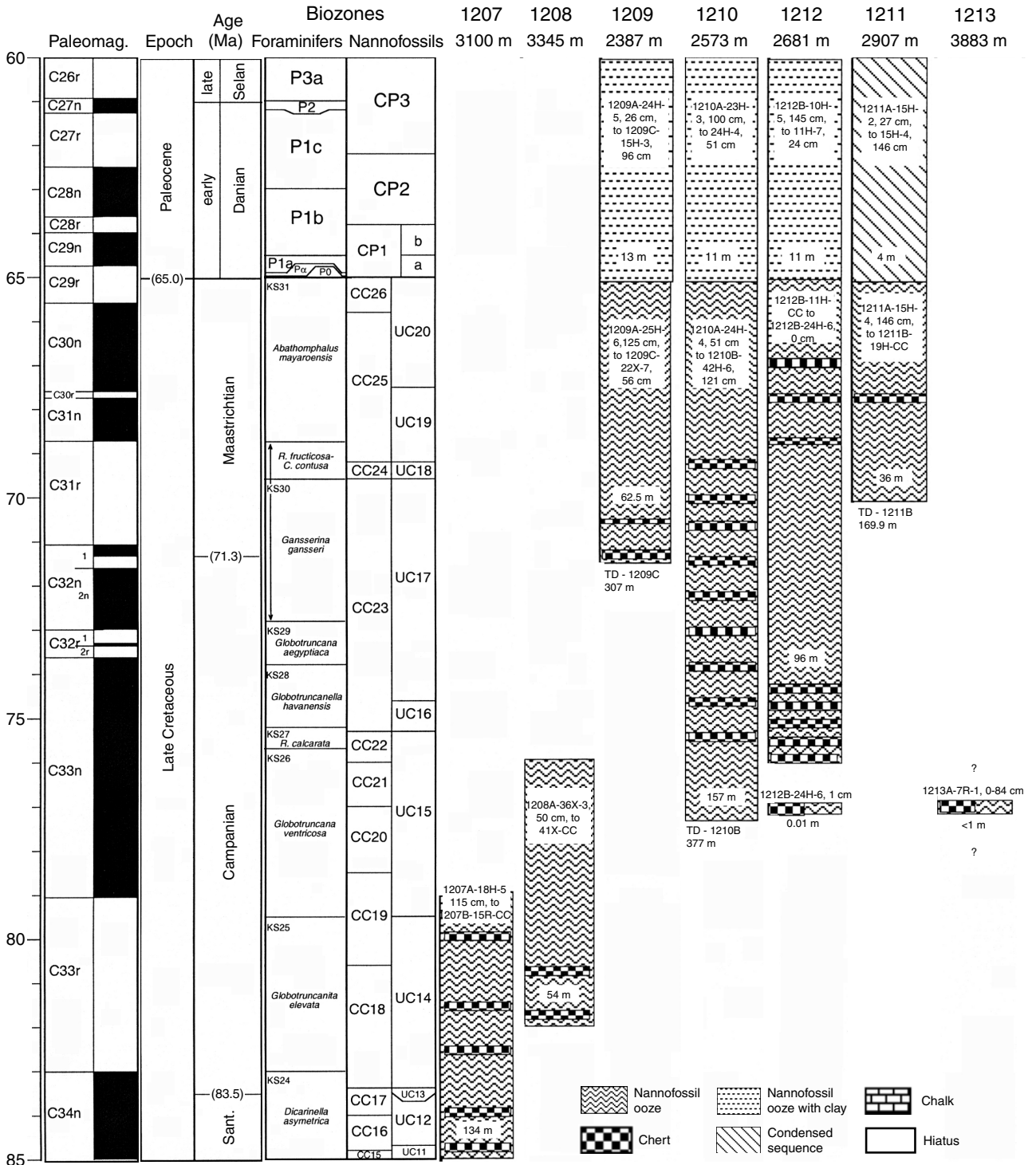
**Figure F7.** Stratigraphic summary for 65–40 Ma. Biostratigraphy after Bralower, Premoli Silva, Malone, et al. (2002), **Bralower** (this volume), **Petrizzo et al.** (this volume), and **Premoli Silva et al.** (this volume). The Paleocene/Eocene boundary was set at 55 Ma (see discussion in Aubry and Ouda, 2003). Condensed pattern annotates intervals in which some biozones could not be identified with certainty and/or may comprise short hiatuses or unconformities. OAE = Ocean Anoxic Event, TD = total depth.
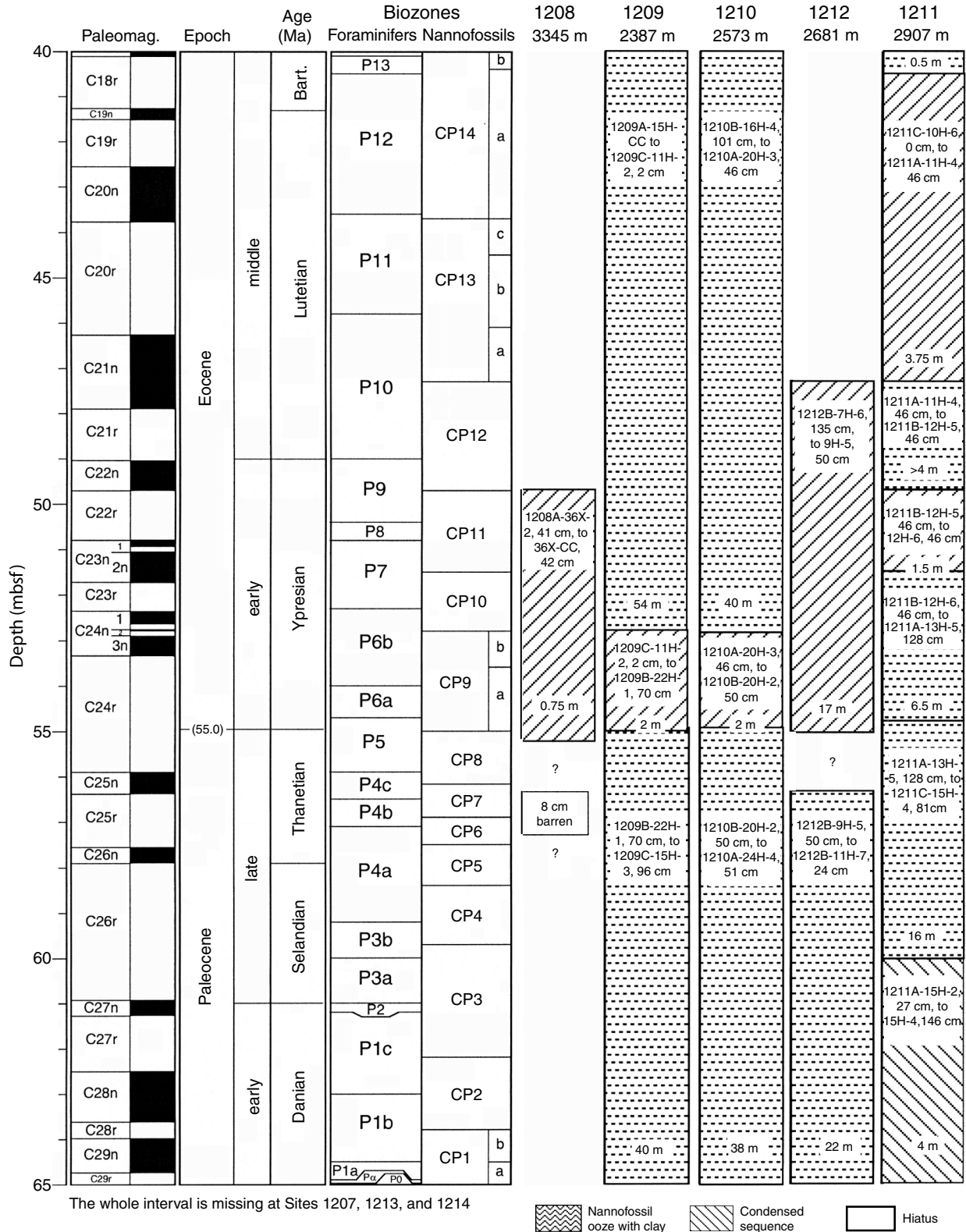
**Figure F8.** Stratigraphic summary for 45–20 Ma. Biostratigraphy after Bralower, Premoli Silva, Malone, et al. (2002), **Bown** (this volume), **Bralower** (this volume), and **Petrizzo et al.** (this volume). Condensed pattern annotates intervals in which some biozones could not be identified with certainty and/or may comprise short hiatuses or unconformities. TD = total depth.
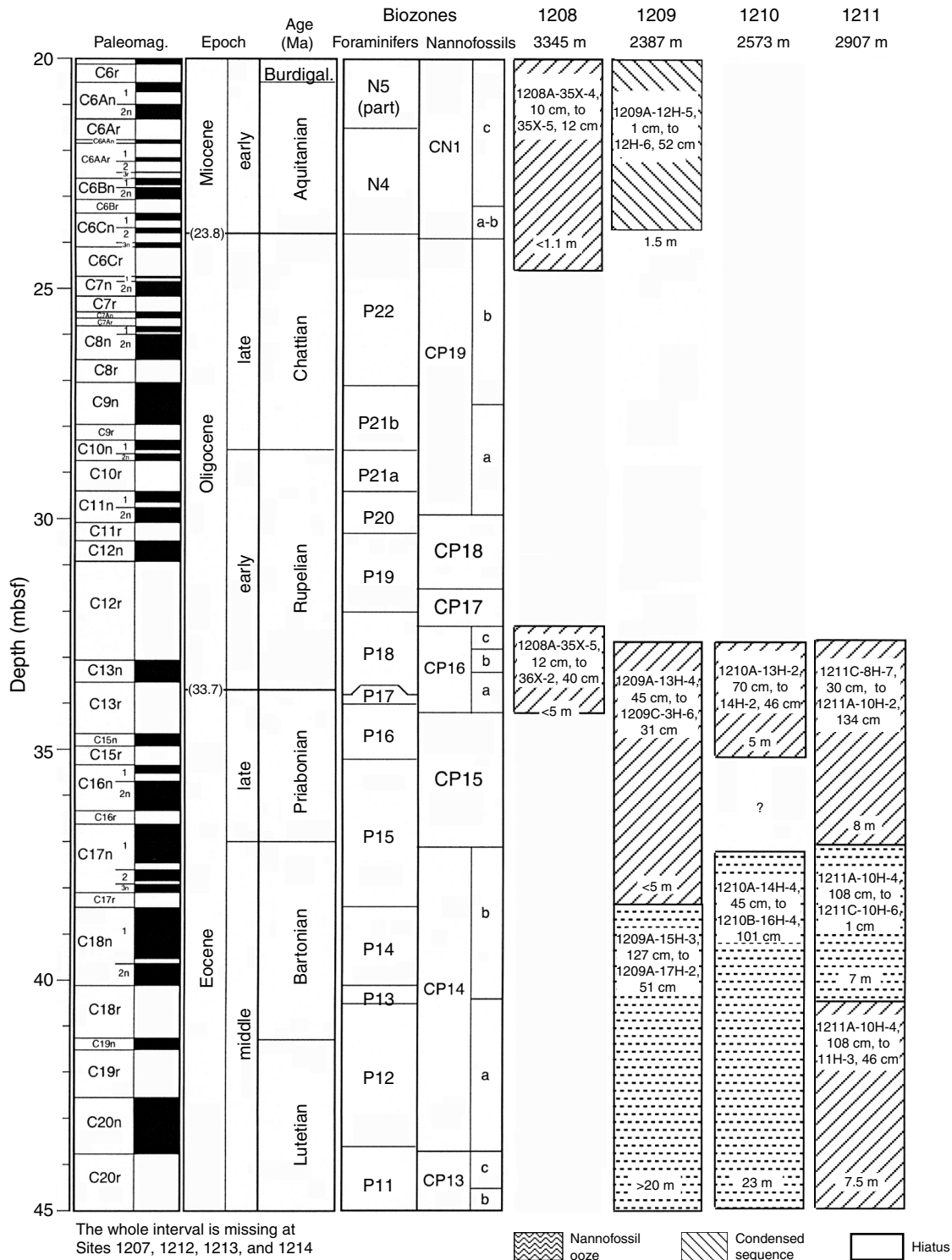
**Figure F9.** Stratigraphic summary for 25–0 Ma. Biostratigraphy after Bralower, Premoli Silva, Malone, et al. (2002) and **Bown** (this volume). Magnetostratigraphy after **Evans et al.** (this volume). Condensed pattern annotates intervals in which some biozones could not be identified with certainty and/or may comprise short hiatuses or unconformities. TD = total depth.
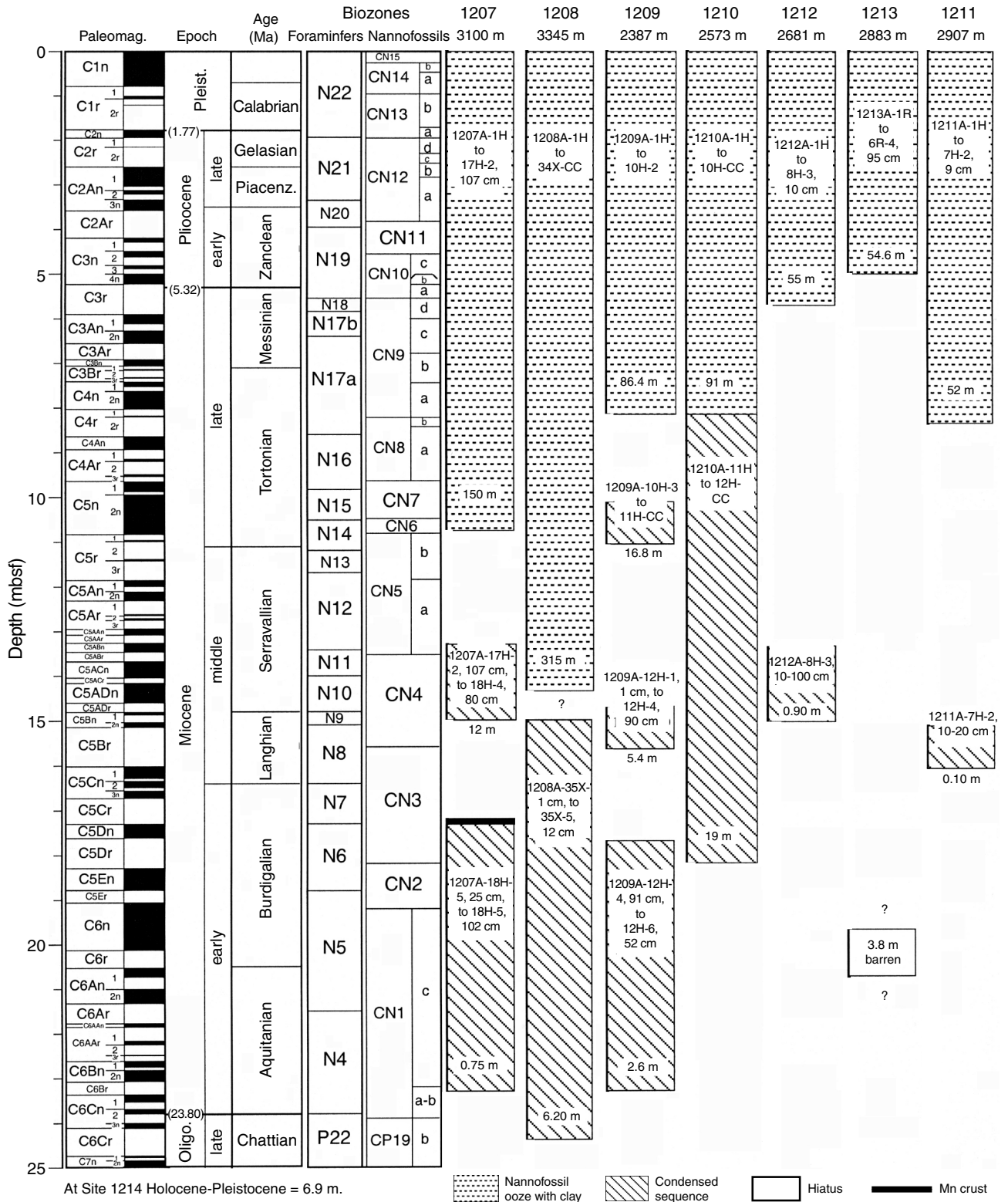
**Figure F10.** Magnetic polarity interpretation of Hole 1213B Lower Cretaceous sediment samples between 360 and 424 mbsf. Solid circles = inclination values for samples; subbottom depth has been recalculated to expand recovered core to fill the cored intervals. Polarity interpretation is shown at right: black = normal polarity, white = reversed polarity, and gray = uncertain polarity (from **Sager et al.,** this volume).
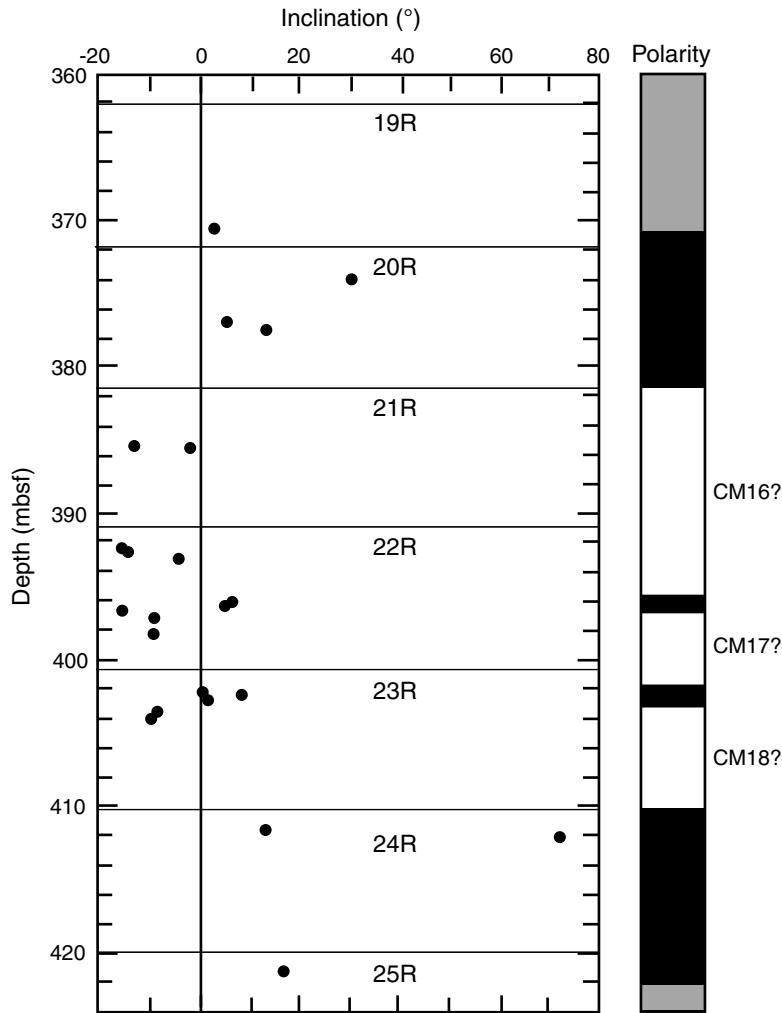
**Figure F11.** Geochemistry of diabase sills recovered at Site 1213. **A, B.** Age-corrected isotope data. Fields for Pacific mid-ocean ridge basalt (MORB) and the Easter-Nazca Ridge hotspot chain are adjusted for radiogenic ingrowth to the estimated 144-Ma positions of the mantle sources (see Tejada et al., 2004). Pb isotope data for Holes 1213B and 1179D (and Easter-Nazca Ridge) were acquired using a double spike. Fields are from Mahoney and Spencer (1991), Tejada et al. (2004), and Ray et al. (2003), and references therein. **C.** Incompatible element patterns. Ontong Java pattern is from Fitton and Godard (2004); average normal-MORB (N-MORB) pattern and normalizing values are Sun and McDonough's (1989) (from Mahoney et al., 2005).
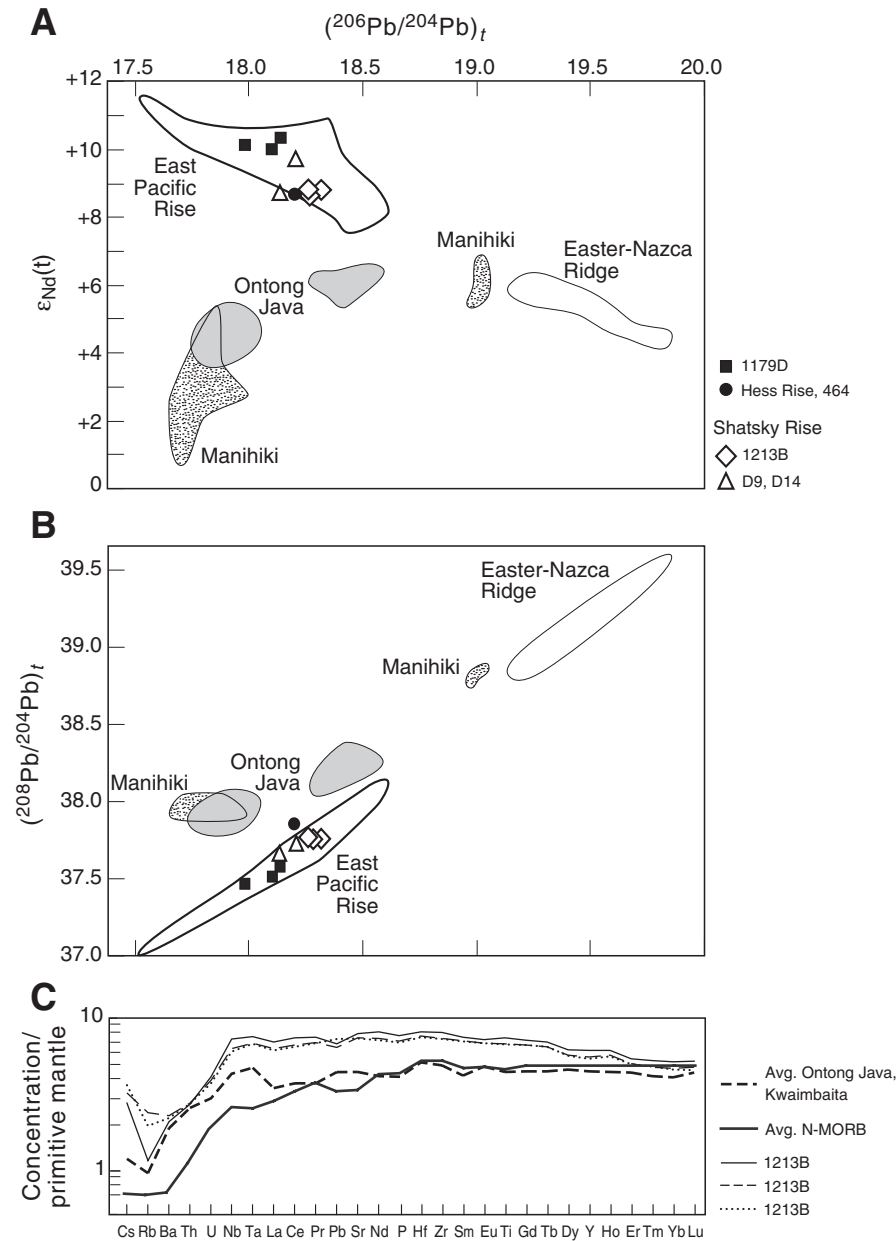
**Figure F12.** Core photo, carbonate, $C_{org}$ contents, and hydrogen index (HI) for lower Aptian sedimentary rocks recovered at Sites 1207, 1213, and 1214. Note that Sites 1207 and 1213 recovered $C_{org}$-rich intervals that represent OAE1a (from Bralower, Premoli Silva, Malone, et al., 2002). NA = not analyzed.



Cores of early Aptian OAE1a interval recovered on Leg 198
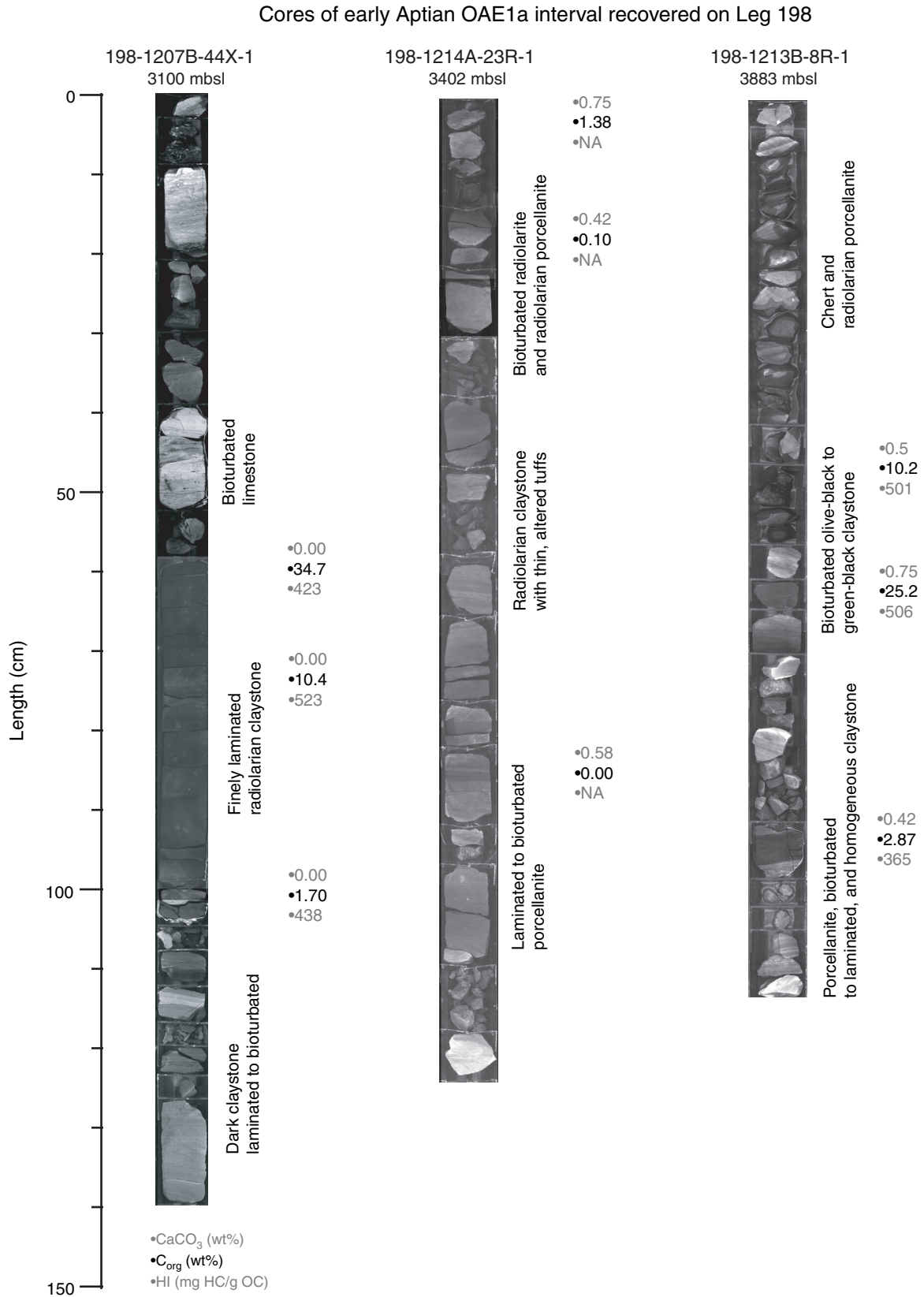
**Figure F13.** Summary of sedimentological interpretations and correlation of Hauterivian–Albian interval between Sites 1207 and 1213. Correlation is based upon nannofossil biostratigraphy and geophysical and lithological data (from Robinson et al., 2004).
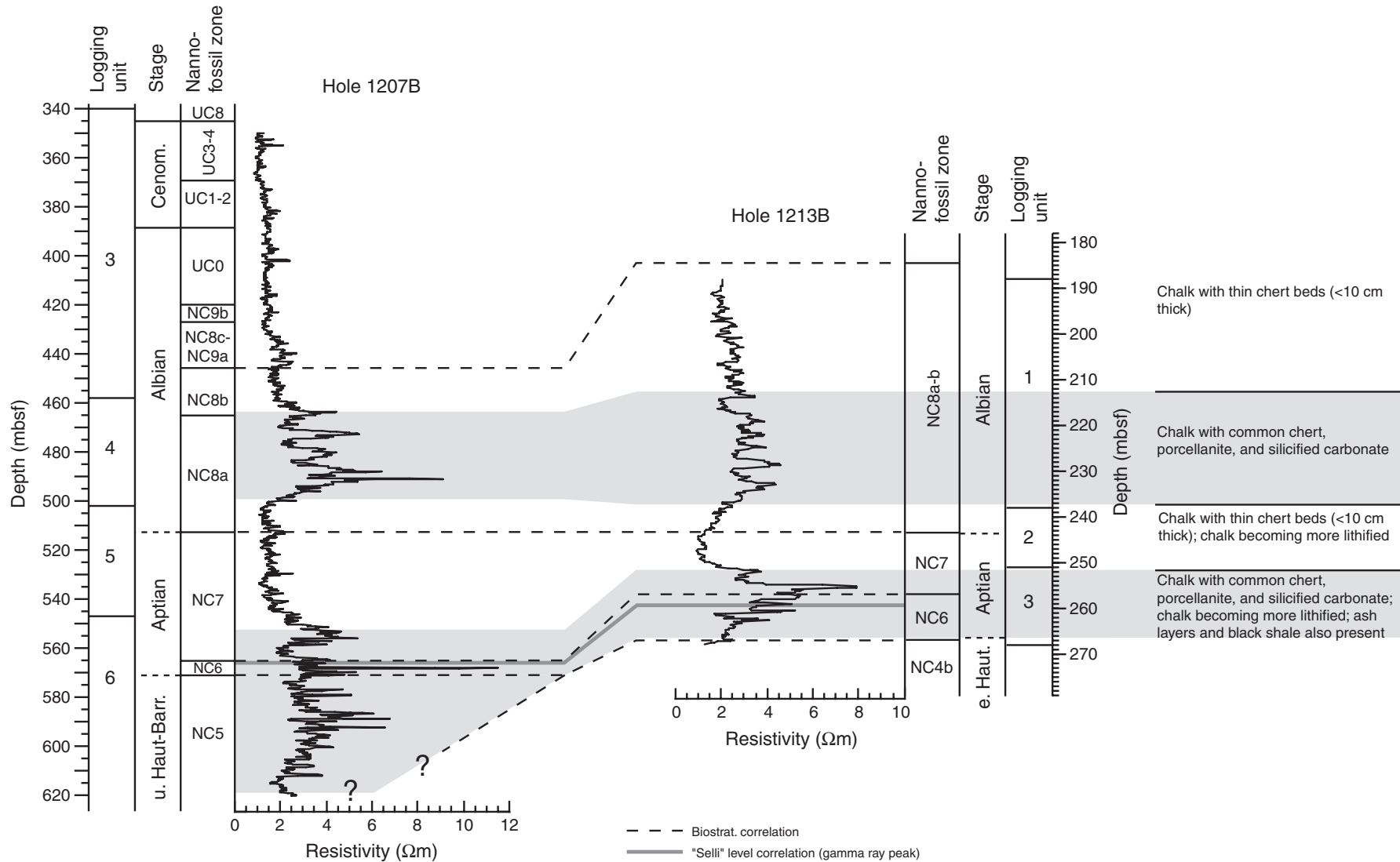
**Figure F14.** Carbon (left column), oxygen (middle column), and neodymium (right column) isotope records for 66–72 Ma interval from Sites 1209, 1210, and 1212. Shaded bars across Site 1209 and 1210 records indicate chronostratigraphic extent of the inoceramid event (from Frank et al., 2005). V-PDB = Vienna Pedee belemnite.
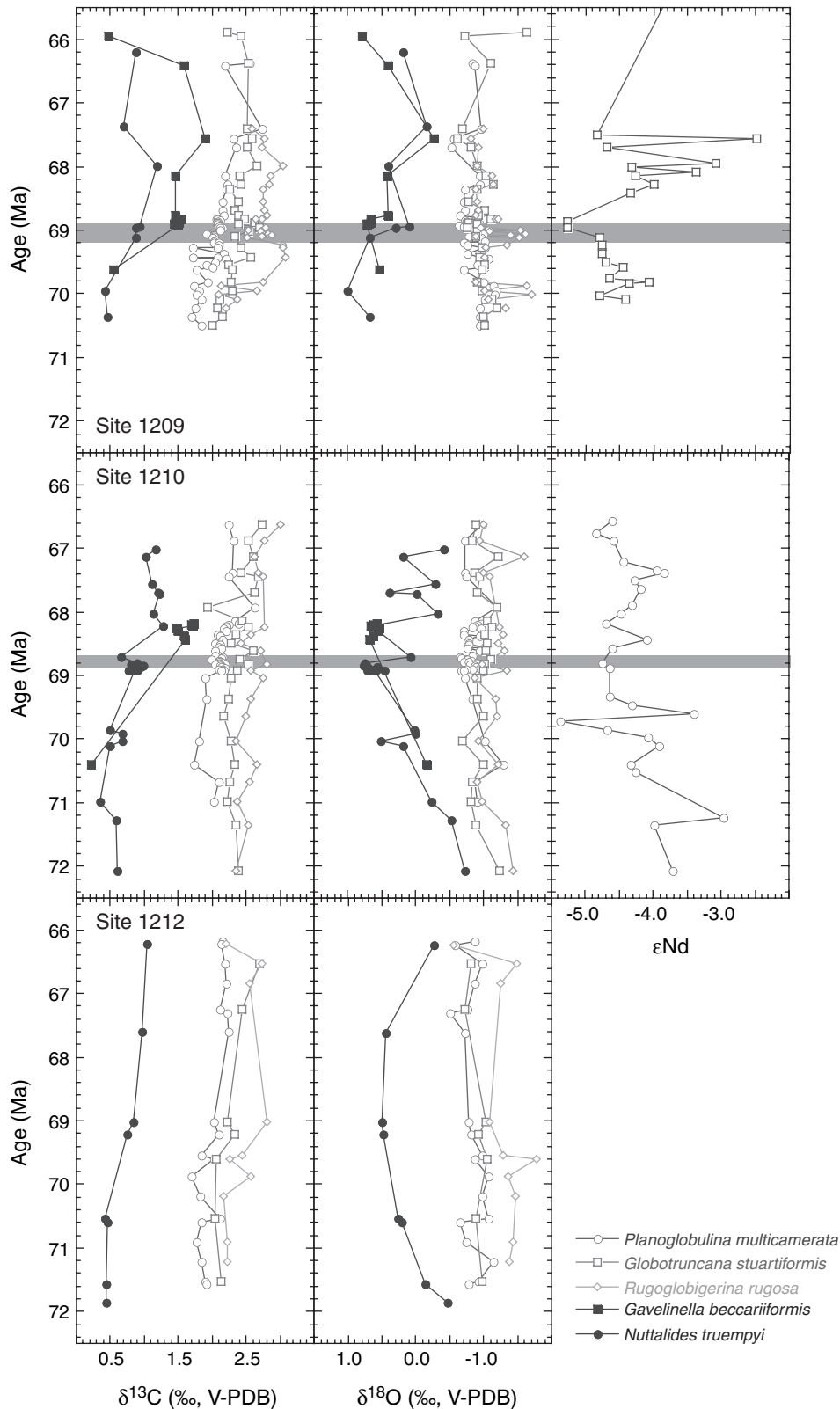
**Figure F15.** Paleogene stable isotope results for foraminifers from Site 1209 in the subtropical Pacific and Site 865 in the equatorial Pacific (Bralower et al., 1995) plotted relative to age using the nannofossil stratigraphies of **Bralower** (this volume) and Bralower and Mutterlose (1995), respectively, relative to the Berggren et al. (1995) timescale. Open squares = surface planktonic Mg/Ca data at Site 865 (Tripati et al., 2003); open circles = surface planktonics; crosses = *Subbotina* spp.; solid circles = benthics. Paleotemperature scales are calculated using the equation of Erez and Luz (1983) with dw of deep water = $\delta_D$ = –0.98‰, and dw of surface water = $\delta_S$ = –0.1‰. SAL = salinity event, HTM = hyperthermal event, PETM = Paleocene/Eocene Thermal Maximum event (from Dutton et al., 2005; **Dutton et al.,** this volume).
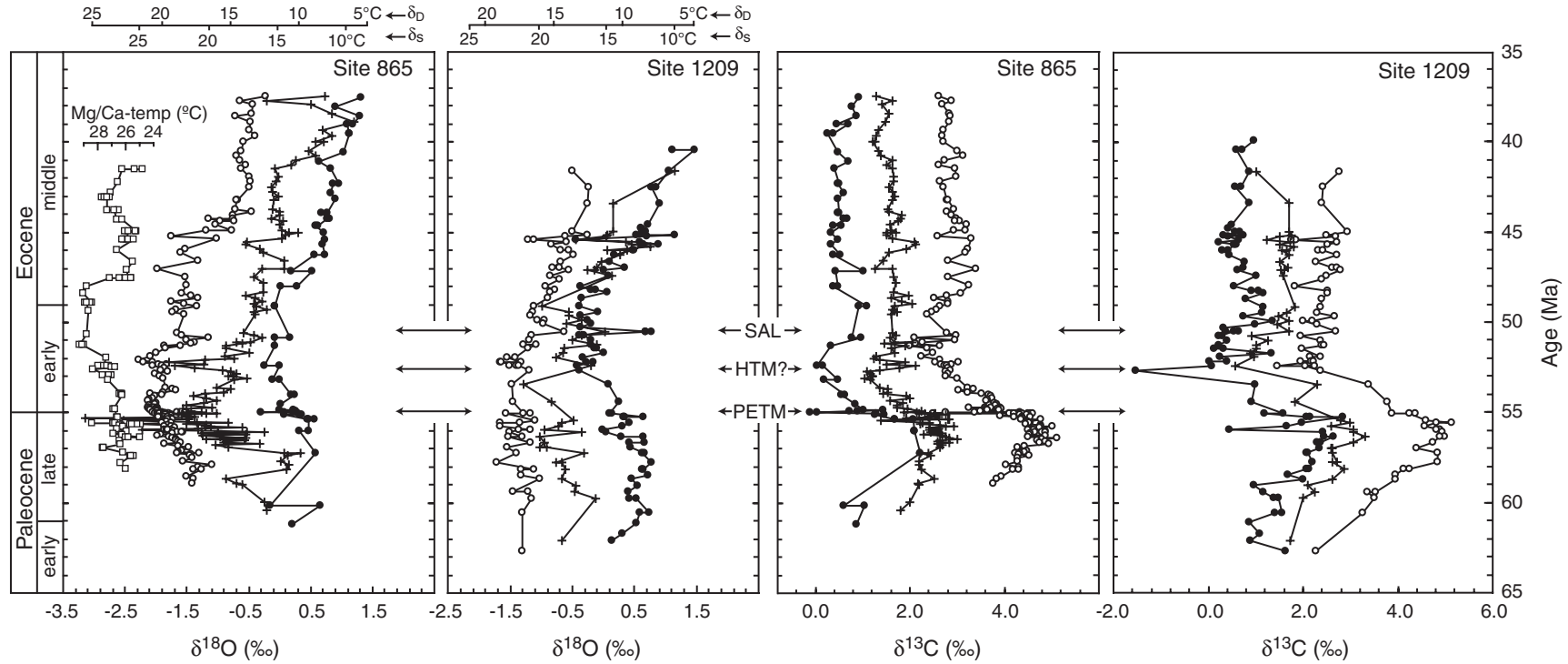
**Figure F16.** Paleogene neodymium isotope records from Sites 1209 and 1211. Diamonds = Site 1209, triangles = Site 1211. Error bars represent two standard deviations. Benthic foraminiferal oxygen isotope values (green dots; from Zachos et al., 2001) provide an estimate of deep-sea temperature. The vertical line represents a deep-sea temperature of 7°C (from Thomas, 2004).
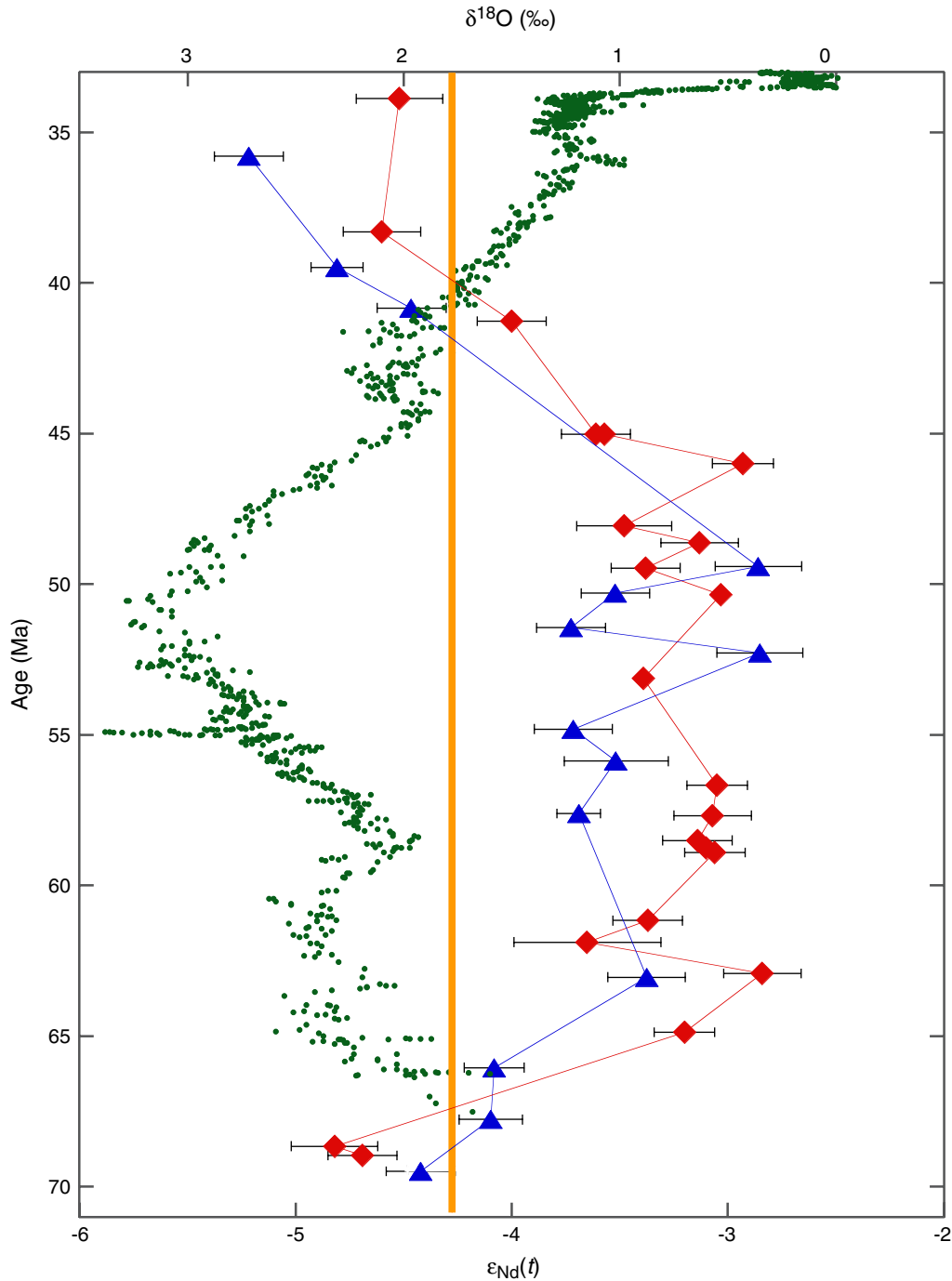
**Figure F17.** Cretaceous/Tertiary boundary sections from Shatsky Rise. Arrows show level of paleontological boundary as recognized by planktonic foraminiferal biostratigraphy (from Bralower, Premoli Silva, Malone, et al., 2002; Bralower et al., 2002; **Premoli Silva et al.,** this volume).
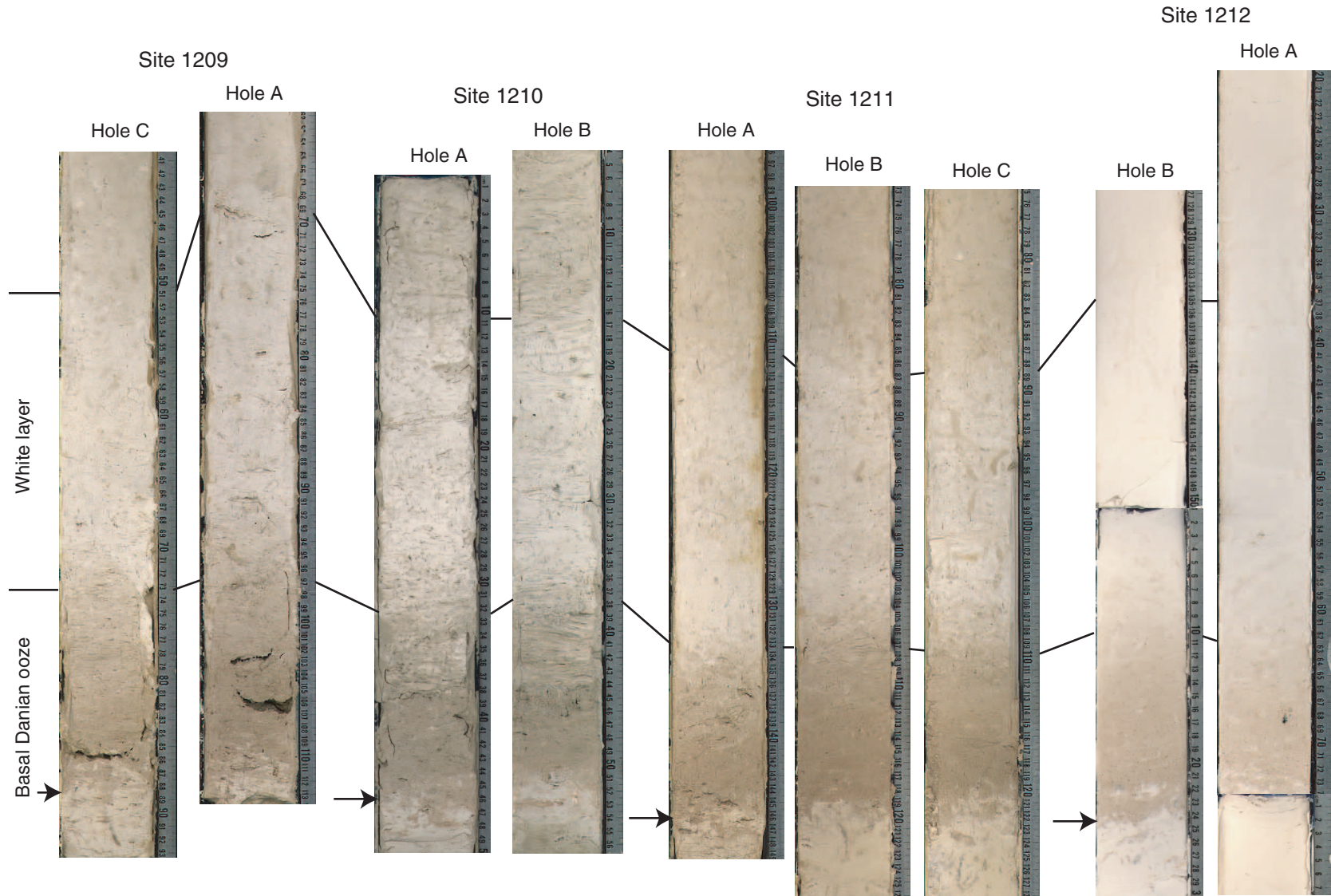
**Figure F18.** Abundances of principal Cretaceous/Tertiary boundary (K/T) survivor and incoming Cenozoic nannofossils. Survivor species counts are percentages of survivor assemblage. Incoming Cenozoic species counts are percentages of total assemblage. Line plots = additional taxa; dashed line = interval of mixed-reworked nannofossil taxa, and heavy dashed line = K/T boundary level (after Bown, 2005).
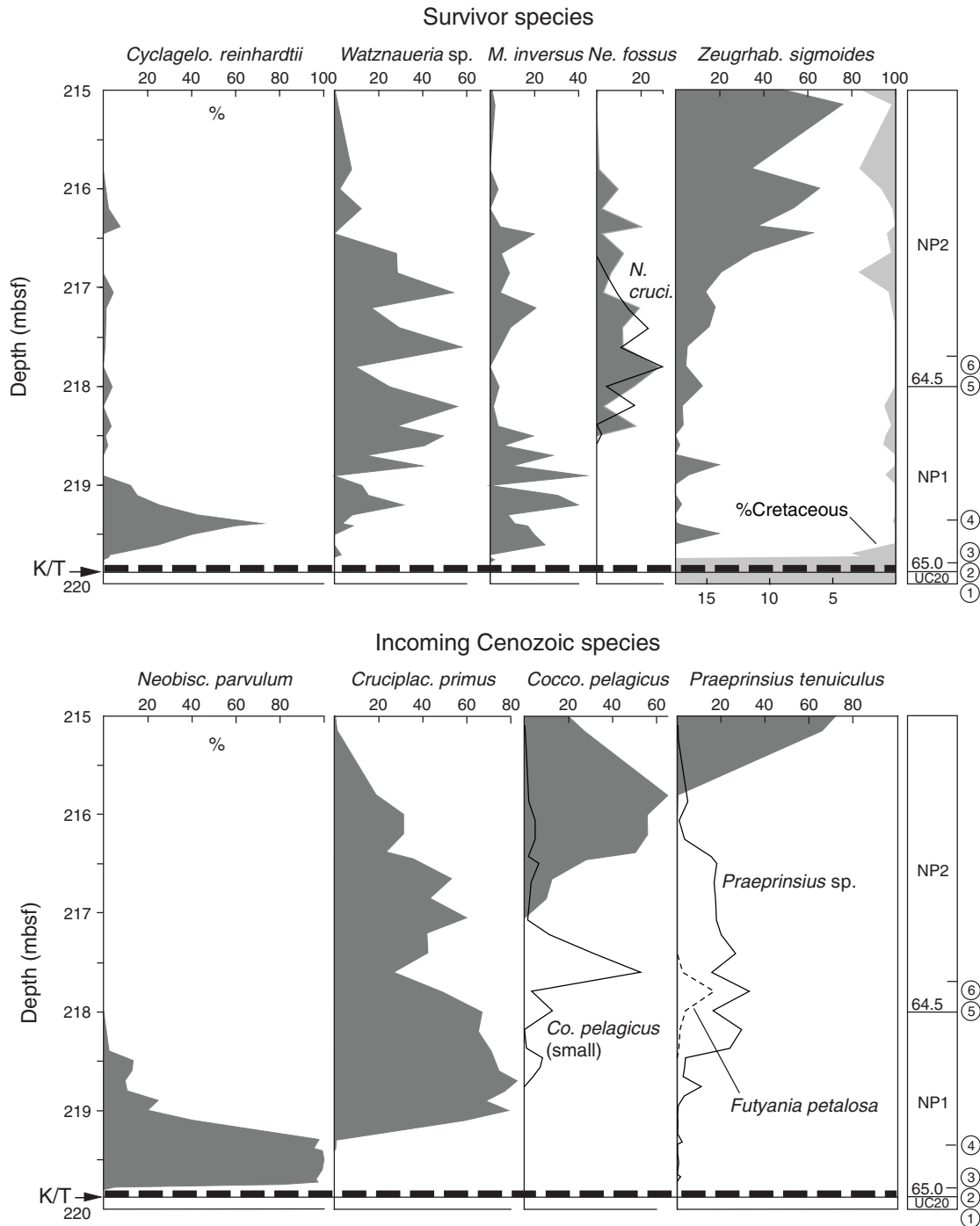
**Figure F19.** The Paleocene/Eocene Thermal Maximum (PETM) sections on Shatsky Rise. Onset of event is recognized by major changes in carbonate content and preservation (confirmed by the presence of bulk sediment carbon isotope excursion). The PETM at Site 1208 is recognized by preservational change and is confirmed by bulk sediment carbon isotope stratigraphy and nannofossil biostratigraphy (**Bown,** this volume). Sites are organized by present (and paleo) water depth.
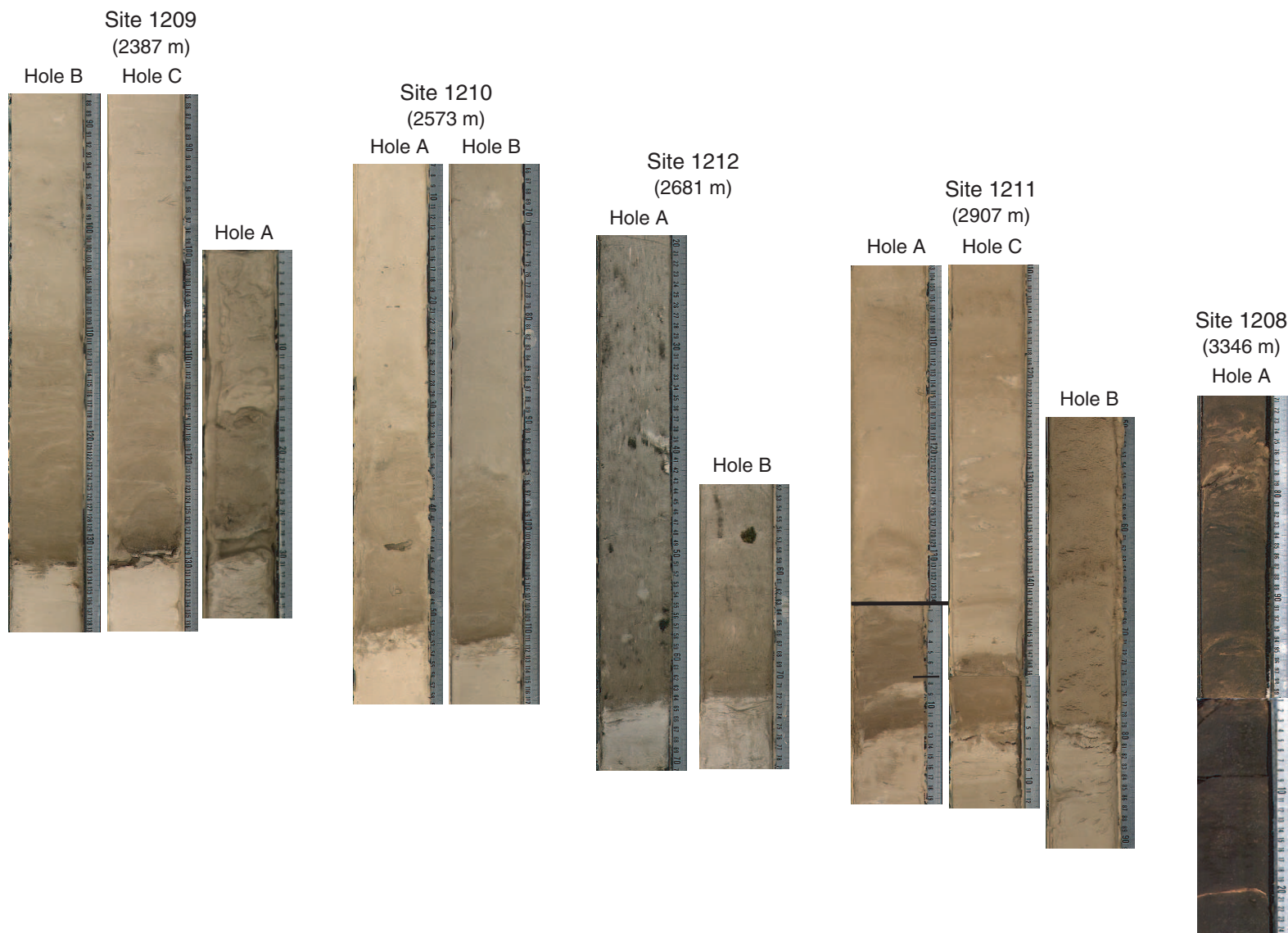
**Figure F20.** Stable isotopes and trace elements from the PETM in Hole 1209B. (**A**) CaCO$_3$ of bulk sediment; (**B**) bulk magnetic susceptibility; (**C**) fragmentation of planktonic foraminifers; (**D, E**) δ$^{13}$C and δ$^{18}$O of individual specimens of *Morozovella velascoensis* (circles) and *Acarinina soldadoensis* (triangles); and (**F, G**) Mg/Ca and Sr/Ca of *Morozovella velascoensis* and *Acarinina soldadoensis* (after Zachos et al., 2003).
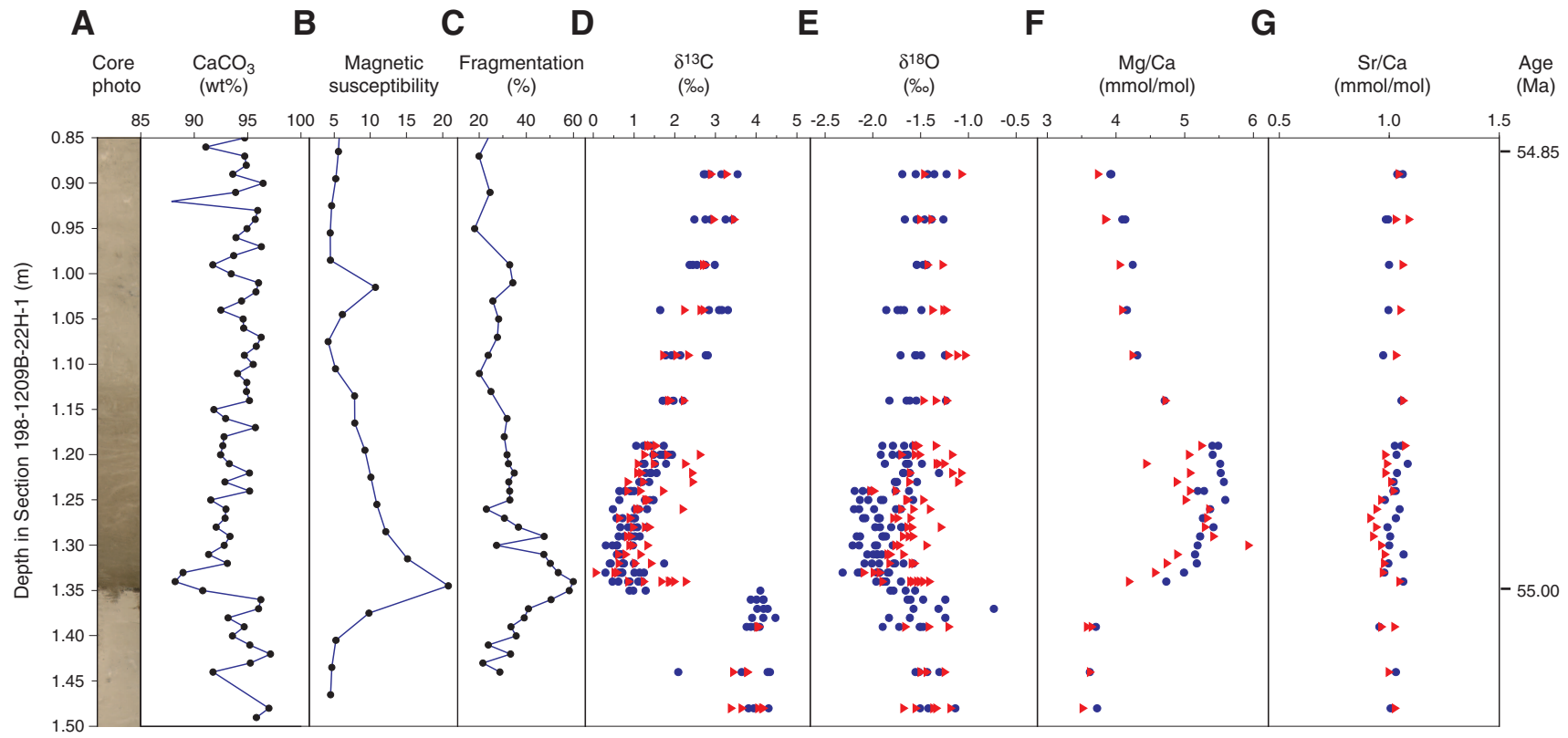
**Figure F21.** Nannofossil diversity and abundance plots for the PETM in Hole 1209B. Nannofossil abundance records are percent abundances relative to the total non-*Toweius-Coccolithus* fraction except for *Toweius* spp. The number of nannofossil fragments relative to 100 whole nannofossils is used as a preservation index. FCO = first common occurrence, LCO = last common occurrence (after Gibbs et al., 2006).
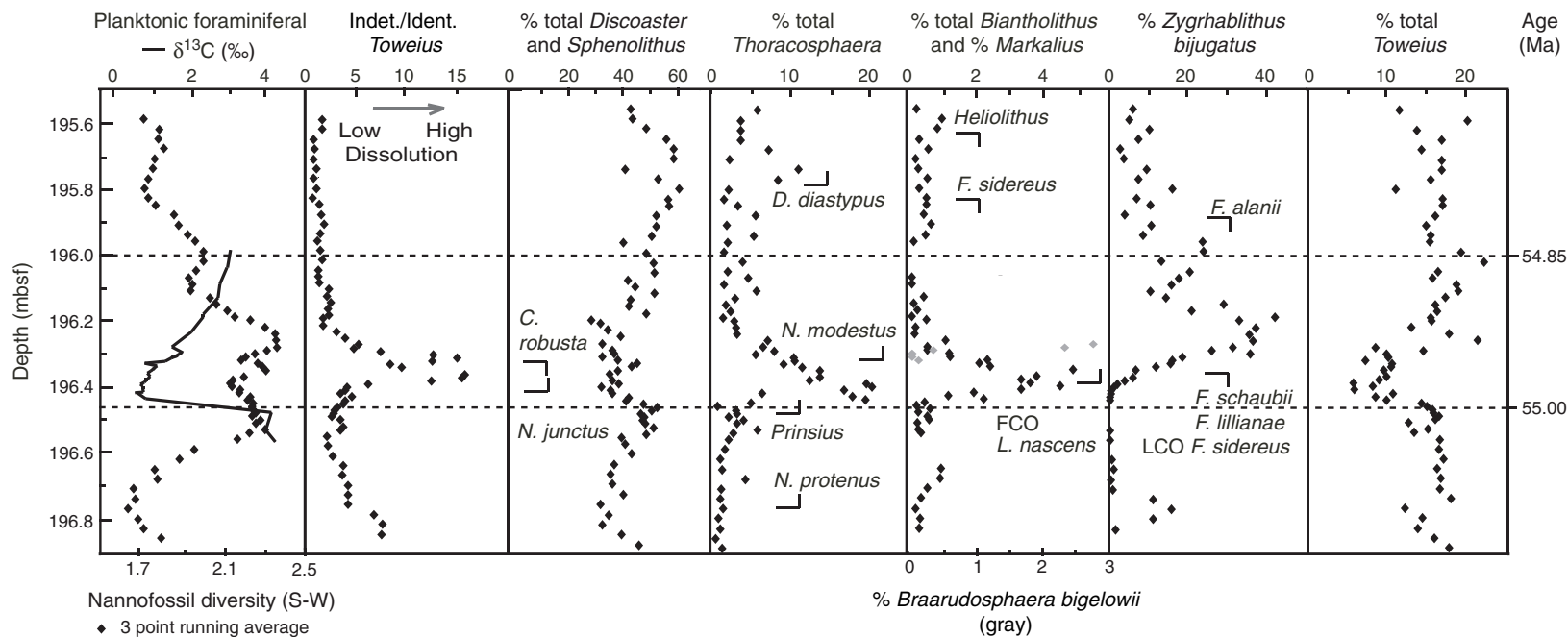
# CHAPTER NOTES

N1. Dumitrescu, M., and Brassell, S.C., submitted. Compositional and isotopic characteristics of organic matter for the early Aptian oceanic anoxic event at Shatsky Rise, ODP Leg 198. *Palaeogeogr., Palaeoclimatol., Palaeoecol.*

N2. Kaiho, K., Takeda, K., Petrizzo, M.R., and Zachos, J.C., submitted. Anomalous shifts in tropical Pacific planktonic and benthic foraminiferal test size during the Paleocene–Eocene Thermal Maximum. *Palaeogeogr., Palaeoclimatol., Palaeoecol.*